Turkish Journal of Earth Sciences (Turkish J. Earth Sci.), Vol. 19, 2010, pp. 239–265. Copyright ©TÜBİTAK
doi:10.3906/yer-0902-9 First published online 17 August 2009

Statistical Evaluation of Classification Diagrams for Altered Igneous Rocks

SURENDRA P. VERMA[1,*], RODOLFO RODRÍGUEZ-RÍOS[2,1,†]
& ROSALINDA GONZÁLEZ-RAMÍREZ[3]

[1] Departamento de Sistemas Energéticos, Centro de Investigación en Energía,
Universidad Nacional Autónoma de México, Temixco, Mor. 62580, Mexico
(E-mail: spv@cie.unam.mx)

[2] (on sabbatical leave from) Facultad de Ingeniería e Instituto de Geología, Universidad Autónoma de San Luis Potosí, Av. Dr. Manuel Nava No. 8, Zona Universitaria, San Luis Potosí, S.L.P. 78240, Mexico

[3] Posgrado en Ingeniería – Energía, Centro de Investigación en Energía,
Universidad Nacional Autónoma de México, Temixco, Mor. 62580, Mexico

[†] Deceased; July 27, 2009

Received 22 January 2009; revised typescript received 15 July 2009; accepted 27 July 2009

Abstract: The International Union of Geological Sciences (IUGS) has proposed recommendations for the classification of relatively fresh volcanic rocks, but with no specific instructions for altered volcanic rocks, other than discouraging the use of the total alkalis versus silica diagram. The Nb/Y-Zr/TiO_2 diagram has been in use for the classification of altered rocks now for over 30 years. Recently (during 2007) another diagram (Co-Th) has been proposed to replace this old diagram, particularly for altered arc rocks. Using an extensive database of all kinds of relatively fresh rocks from four tectonic settings (island arc, continental rift, ocean island, and mid-ocean ridge), as well as from three settings excluding island arc, we carried out an objective evaluation of the old Nb/Y-Zr/TiO_2 diagram for rock classification. Similarly, for the evaluation of the new Co-Th diagram, an extensive database of similar rocks from island arcs, the Andean active continental margin, continental rifts, ocean islands, and the Mexican Volcanic Belt, was used. Statistical parameters of correct classification or success rate and minimum misclassification defined in this work, respectively, were used to evaluate these diagrams. Our results of the quantification of these parameters showed that none of these diagrams seems to work precisely for the classification of fresh rocks. It is therefore difficult to imagine that they would work well for the classification of altered rocks. Thus, there is an urgent need to apply correct statistical methodology for handling compositional data in proposing new classification diagrams that could provide classification and nomenclature to altered volcanic rocks fully consistent with the IUGS nomenclature for fresh rocks.

Key Words: TAS classification, volcanic rocks, plutonic rocks, chemical classification, correct statistical analysis of compositional data

Altere Magmatik Kayalar İçin Kullanılan Sınıflandırma Diyagramlarının İstatistiksel Değerlendirmesi

Özet: Altere olmayan taze volkanik kayaların sınıflandırması için Uluslararası Jeoloji Bilimleri Birliği'nin (The International Union of Geological Sciences, IUGS) önerdiği kayaların toplam alkali ve silis bileşimlerinin kullanımı dışında, altere volkanik kayaların sınıflandırılmasında kullanılacak bir yönerge henüz bulunmamaktadır. Altere olmuş volkanik kayaların sınıflandırılmasında son 30 yılı aşkındır Nb/Y-Zr/TiO_2 diyagramı kullanılmaktadır. Son olarak 2007'de, bu diyagrama alternatif olarak altere volkanik kayaların Co ve Th içeriklerini kullanan başka bir diyagram önerilmiştir. Bu çalışmada ada yayları, kıtasal riftler, okyanus adaları ve okyanus ortası sırtlar olmak üzere 4 farklı tektonik ortamdan ve ayrıca ada yayları hariç olmak üzere 3 tektonik ortama ait tüm kaya çeşitlerinden elde edilen geniş bir veri tabanı kullanılarak Nb/Y-Zr/TiO_2 diyagramı değerlendirilmiştir. Yeni önerilen Co-Th diyagramını değerlendirmek için, aynı yöntemle ada yaylarından, And-tipi aktif kıta kenarından, kıtasal riftlerden, okyanus

adalarından ve Meksika Volkanik Kuşağı'ından benzer kayalara ait veri tabanı kullanılmıştır. Doğru sınıflama veya doğruluk oranı ve yanlış sınıflandırmalara yönelik istatistiksel parametreler tanımlanmış ve diyagramların değerlendirmesinde kullanılmıştır. Bu parametrelerin sayısal sonuçları, bu diyagramlardan hiç birinin taze kayaların sınıflandırılmasında kullanışlı olmadığını göstermiştir. Bu nedenle, altere kayalar için kullanışlı olmalarını beklemek oldukça zordur. Böylece altere kayaların isimlendirmesi ve sınıflandırmasında, taze kayaların IUGS isimlendirmesiyle uyumlu olacak şekilde kullanılabilecek yeni sınıflama diyagramlarının tasarımında kullanılacak doğru istatistiksel yöntemlerin uygulanması gerekmektedir.

Anahtar Sözcükler: TAS sınıflandırması, volkanik kayalar, plütonik kayalar, kimyasal sınıflandırma, bileşimsel verilerin doğru istatistiksel analizi

Introduction

Classification and nomenclature in any science are fundamental issues, because the accuracy of the language used for communication in that particular science depends on them. For the classification of relatively fresh igneous rocks, the International Union of Geological Sciences (IUGS) has made specific recommendations for assigning rock names that depend on their mineralogical and chemical characteristics (Le Bas *et al.* 1986; Le Bas 2000; Le Maitre *et al.* 2002). The well-known TAS (total alkalis *versus* silica; Le Bas *et al.* 1986) diagram seems to be the most popular and widely used for the classification of volcanic rocks. Verma *et al.* (2002) presented a computer program (SINCLAS) to be used for the IUGS volcanic rock classification scheme, which facilitated the application of the TAS diagram as well as providing a standard way of calculating the CIPW norm (Verma *et al.* 2003). In fact, the classification of volcanic rocks and their nomenclature depend on both concepts – the TAS diagram and the CIPW norm (Le Maitre *et al.* 2002; Verma *et al.* 2002). However, the IUGS failed to provide any specific recommendations for the classification of altered rocks, other than discouraging the use of their procedure for relatively fresh rocks for this purpose (Le Bas *et al.* 1986).

In the published literature, some diagrams (alternative to the TAS diagram) have long been proposed, using the so-called immobile elements (Floyd & Winchester 1975, 1978; Winchester & Floyd 1976, 1977), which have been cited in thousands of published papers. In fact, these diagrams, particularly the Nb/Y–Zr/TiO_2 diagram of Winchester & Floyd (1977), have been in wide use even today. Just to name a few references during 2007–2008, we can cite: Gökten & Floyd (2007); Shekhawat *et al.* (2007); Ahmad *et al.* (2008); Bağcı *et al.* (2008); Gladkochub *et al.* (2008); Gürsü (2008); Kadir *et al.* (2008); Keskin *et al.* (2008); Kalmar & Kovacs-Palffy (2008); Kaygusuz *et al.* (2008); Mondal *et al.* (2008); Nardi *et al.* (2008); Pandarinath *et al.* (2008); Wang *et al.* (2008); Yiğitbaş *et al.* (2008); and Zheng *et al.* (2008). On the other hand, others, such as Sheth & Melluso (2008), have used the SINCLAS program for the TAS classification.

More recently, the subject of the classification of altered rocks has been revived through the publication of a paper by Hastie *et al.* (2007) who stated that the existing diagrams did not work well for arc rocks and proposed, more specifically, the use of Co-Th diagram for the classification of altered rocks from volcanic arcs.

The question arises if these older (Floyd & Winchester 1975, 1978; Winchester & Floyd 1976, 1977) and the most recent (Hastie *et al.* 2007) diagrams 'correctly' classify altered rocks. We cannot precisely answer this question by studying altered rocks because we do not know how much their chemical composition was modified by alteration processes in the field. We could, of course, resort to experimental laboratory-controlled work to answer it, which would also be costly, time consuming, and difficult due to the multivariate nature of this problem. Therefore, we adopted the philosophy of objectively testing the functioning of these diagrams using data for fresh volcanic rocks from different areas and tectonic settings. If the classification diagrams were shown to work well for fresh rocks, i.e., if they showed that high percentages of fresh rocks are named correctly and consistently with the IUGS classification scheme (combination of the TAS diagram and CIPW norm), we could expect that they might work well for altered rocks as well, provided

that the concentrations of the chemical elements used in these diagrams were not significantly modified during the alteration. Thus, the percentages of correct classification in such diagrams would probably represent approximately the maximum percentages of correct classification for altered rocks.

With this philosophy in mind, the following methodology was applied for the present evaluation: (a) compile databases for fresh volcanic rocks from different tectonic settings; (b) separate samples of a given rock type from the compiled databases; (c) plot samples of a particular rock type in the diagram to be evaluated and determine the new rock names; (d) count samples of each new rock name as classified in the evaluated diagram; (e) calculate statistical information about the percentages of each new rock type in terms of the original samples of that particular rock type being evaluated; (f) repeat this procedure for all rock types from the IUGS classification scheme; and (g) report the results in figures and tables and point out their implications.

Specifically, two diagrams –the old Nb/Y–Zr/TiO_2 diagram of Winchester & Floyd (1977) and the new Co-Th diagram of Hastie *et al.* (2007) – were evaluated in detail. The results clearly show that neither of them works satisfactorily, highlighting thus the urgent need of proposing new, more efficient diagrams, for which the statistically correct methodology for handling compositional data must be used.

Databases

The data were compiled from all Miocene to Recent rock types from different areas of known, uncontroversial tectonic settings from all over the world. Initially, databases from island arcs, continental rifts, ocean islands, and mid-ocean ridges, as well as from the Mexican Volcanic Belt (MVB) and the Andean continental arc, were established and used by Verma & Aguilar-Y-Vargas (1988); Verma (1997, 2000a,b, 2002, 2004, 2006, 2009a, 2010; Verma (2000); Vasconcelos-F. *et al.* (1998, 2001), Agrawal *et al.* (2004, 2008); Verma *et al.* (2006); and Agrawal & Verma (2007). An updated version of these databases was prepared and used for the present work. Specifically, Verma *et al.* (2006) presented the information on the number of samples, their tectonic setting and location coordinates, and literature references. Later, Agrawal *et al.* (2008) stated that Electronic Annexure EA-1, with such information on additional samples compiled by them, is available upon request from the authors. Additional details are given in a companion paper by Verma (2010). Therefore, to avoid repetition these details are omitted from the present paper.

All data, except those from the MVB and the Andes, were used to evaluate the old Nb/Y–Zr/TiO_2 diagram by Winchester & Floyd (1977). Furthermore, a second evaluation of this old diagram was also carried out using rocks from only three tectonic settings of continental rift, ocean island and mid-ocean ridge.

For the evaluation of the new Co–Th diagram by Hastie *et al.* (2007), data from island arcs, continental rifts, and ocean islands as well as the MVB and the continental arc of the Andes were used separately. MORB data were not used here because, as expected, our compilation for this setting was mostly of basic rocks, and we wanted to cover all rock types from a given tectonic setting. The Andes data were an updated version of the compilation by Verma *et al.* (2006).

The rock names of all compiled rocks were ascertained using the SINCLAS computer program (Verma *et al.* 2002, 2003), which also provided standard igneous norms according to the IUGS recommendations (Le Bas *et al.* 1986; Le Bas 2000; Le Maitre *et al.* 2002). Note that SINCLAS also provides adjusted data (identified here as the subscript $_{adj}$) on an anhydrous 100% basis with a prior adjustment of Fe-oxidation ratio. The rest of the methodology was the same as outlined above in the Introduction section.

Results

The results are arranged in two following subsections.

Old Classification Diagrams

Floyd & Winchester (1975, 1978) and Winchester & Floyd (1976, 1977) presented several diagrams for

the classification of altered rocks. These were of the following three types; (1) element-element: (i) Zr-P_2O_5; and (ii) Zr-TiO_2; (2) element-element ratio: (iii) Ce-Zr/TiO_2; (iv) Ga-Zr/TiO_2; (v) Zr/TiO_2-SiO_2; (vi) Nb/Y-SiO_2; (vii) Y/Nb-TiO_2; and (viii) Zr/P_2O_5-TiO_2; and (3) element ratio-element ratio: (ix) Nb/Y-Zr/TiO_2; (x) Nb/Y-Ga/Sc; and (xi) Zr/P_2O_5-Nb/Y.

Several diagrams – (i) Zr-P_2O_5; (ii) Zr-TiO_2; (vii) Y/Nb-TiO_2; (viii) Zr/P_2O_5-TiO_2; (ix) Nb/Y-Zr/TiO_2; and Zr/P_2O_5-Nb/Y– were proposed (Floyd & Winchester 1975; Winchester & Floyd 1976) to distinguish only two types of basaltic rocks – tholeiitic and alkali. The term tholeiite has not been recommended by the IUGS (Le Bas *et al.* 1986; Le Bas 2000; Le Maitre *et al.* 2002). Because for this evaluation we wanted to strictly follow the IUGS recommendations for the rock classification and nomenclature, it was not possible to separate tholeiites from alkali basalt in our database using the IUGS scheme. Therefore, these diagrams cannot be evaluated using the IUGS nomenclature as the reference frame for our work.

The diagrams (v) Zr/TiO_2-SiO_2 and (vi) Nb/Y-SiO_2 (Winchester & Floyd 1977; Floyd & Winchester 1978), both involving SiO_2 and having been proposed to classify all volcanic rock types, are also not worth evaluating for several reasons. Firstly, they involve one of the same axes, viz., SiO_2, of the TAS diagram. The names inferred from Zr/TiO_2-SiO_2 and Nb/Y-SiO_2 are likely to be similar to the TAS diagram, because in both the subdivision basalt-andesite-dacite-rhyolite depends on the SiO_2 content. However, the subdivision proposed by Winchester & Floyd (1977) does not fully match with that of the IUGS (Le Bas *et al.* 1986), for example, in the former, basaltic andesite is absent and rhyodacite is present. These differences will be simply reflected in the evaluation. Secondly, SiO_2 may also be somewhat variable under alteration processes, for example, under geothermal conditions (e.g., Fournier & Potter II 1982; Verma & Santoyo 1997; M.P. Verma 2000; Torres-Alvarado 2002; Pandarinath *et al.* 2006; Torres-Alvarado *et al.* 2007). Silica is known to dissolve from rocks –especially from basic rocks– during interaction with water at greater temperatures than those of the surface ambient conditions. This is why the well known silica geothermometers actually work for inferring subsurface temperatures in geothermal systems (e.g., Fournier & Potter II 1982; Verma & Santoyo 1997; Díaz-González *et al.* 2008; Palabıyık & Serpen 2008; Verma *et al.* 2008a). Finally, because the classification depends on both axes, the other parameter –Zr/TiO_2 or Nb/Y– might affect the rock names if they are not perfect proxies for total alkalis. The behaviour of these two ratio variables can be better evaluated in the Nb/Y-Zr/TiO_2 diagram (see below).

Winchester & Floyd (1977) also presented (iii) Ce-Zr/TiO_2 and (iv) Ga-Zr/TiO_2 diagrams for rock classification. However, they also noted that these diagrams did not perform so well as the Nb/Y-Zr/TiO_2 diagram, because different basalt types and basanite were not clearly distinguished and, for subalkaline magmas, neither Ce nor Ga showed any significant increase with differentiation, i.e., no significant change with increasing SiO_2. Consequently, although these authors presented these two diagrams, they did not recommend their use for rock classification purposes.

The 10th diagram –(x) Nb/Y-Ga/Sc– proposed by Winchester & Floyd (1977), was also not evaluated because the authors noted that the data, on which this diagram was based, were particularly scarce and the classification boundaries were not definitive. No new boundaries were later proposed by these authors. Besides, the functioning of the Nb/Y parameter will be evaluated in the Nb/Y-Zr/TiO_2 diagram.

Thus, in spite of almost a dozen of these old diagrams, only the Nb/Y-Zr/TiO_2 diagram of Winchester & Floyd (1977) –henceforth called, for simplicity, the W&F diagram– was evaluated in this work. The results are presented in Figures 1–7. The numbers of the IUGS (TAS+CIPW norm) classified samples for each rock type as well as those of the W&F diagram classified samples were calculated. Thus, for a given IUGS rock name, the total number of samples was identified and assumed to represent 100%. The numbers of samples plotting in all fields of the W&F diagram were divided by the initial number of samples of that particular rock type used for the evaluation and the ratios were expressed as percentages of W&F classification. When the W&F

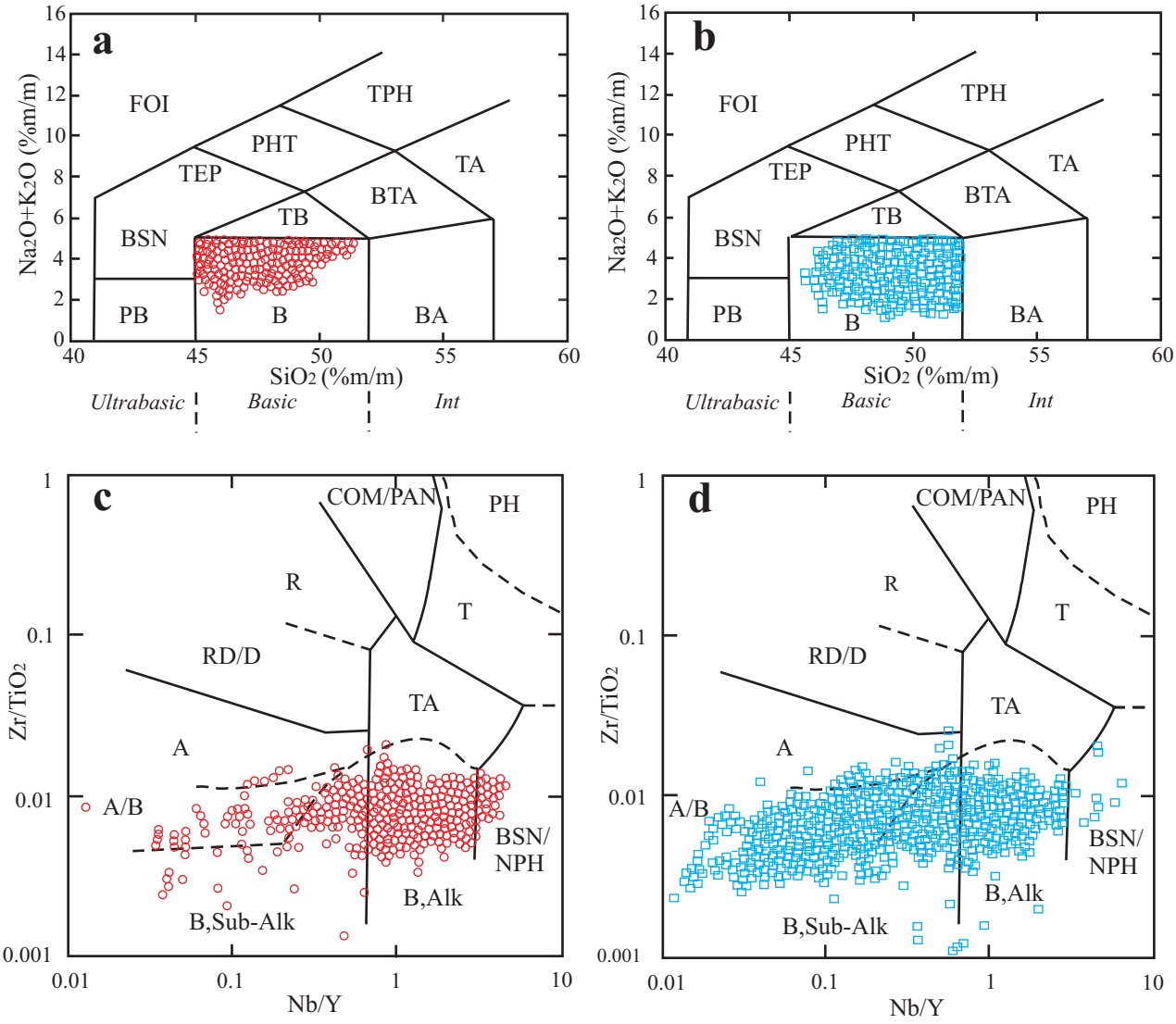

Figure 1. Statistical evaluation of the Nb/Y-Zr/TiO_2 diagram (Winchester & Floyd 1977) –called the W&F diagram in this work– in reference to the TAS (total alkalis *versus* silica) diagram (Le Bas *et al.* 1986; Verma *et al.* 2002) of the IUGS classification scheme, using basaltic rocks from our database. Note also that the IUGS recommendation to use adjusted data in the TAS diagram was strictly followed (Verma *et al.* 2002). The field names in the TAS diagram, viz., (a) and (c), are: PB– picrobasalt; B– basalt; BA– basaltic andesite; BSN– basanite; TEP– tephrite; TB– trachybasalt; BTA– basaltic trachyandesite; TA– trachyandesite; FOI– foidite; PHT– phonotephrite; and TPH– tephriphonolite. Only part of the TAS diagram is shown. Other TAS rock names not included in this diagram, but present in some later Figures are: PH– phonolite; A– andesite; D– dacite; TD– trachydacite; T– trachyte; R– rhyolite. Similarly, for the W&F diagram, viz., (b) and (d), the field names are: B,Alk– alkali-basalt; B,Sub-Alk–Sub-alkaline basalt; BSN/NPH– basanite/nephelinite; B/A– basalt/andesite; A– andesite; TA– trachyandesite; T– trachyte; PH– phonolite; COM/PAN– comendite/pantellerite; RD/D– rhyodacite/dacite; and R– rhyolite. The same symbols are used in the W&F diagram as in the corresponding TAS diagram, i.e., the symbols are the same in the **(a)** and **(c)** pairs of diagrams and **(b)** and **(d)** pairs. **(a)** Alkali basalt (650) samples according to the TAS diagram; **(b)** subalkaline basalt (1200) samples according to the TAS diagram; **(c)** the same alkali basalt (650) samples of the TAS diagram plotted in the W&F diagram; and **(d)** the same subalkaline basalt (1200) samples of the TAS diagram plotted in the W&F diagram.

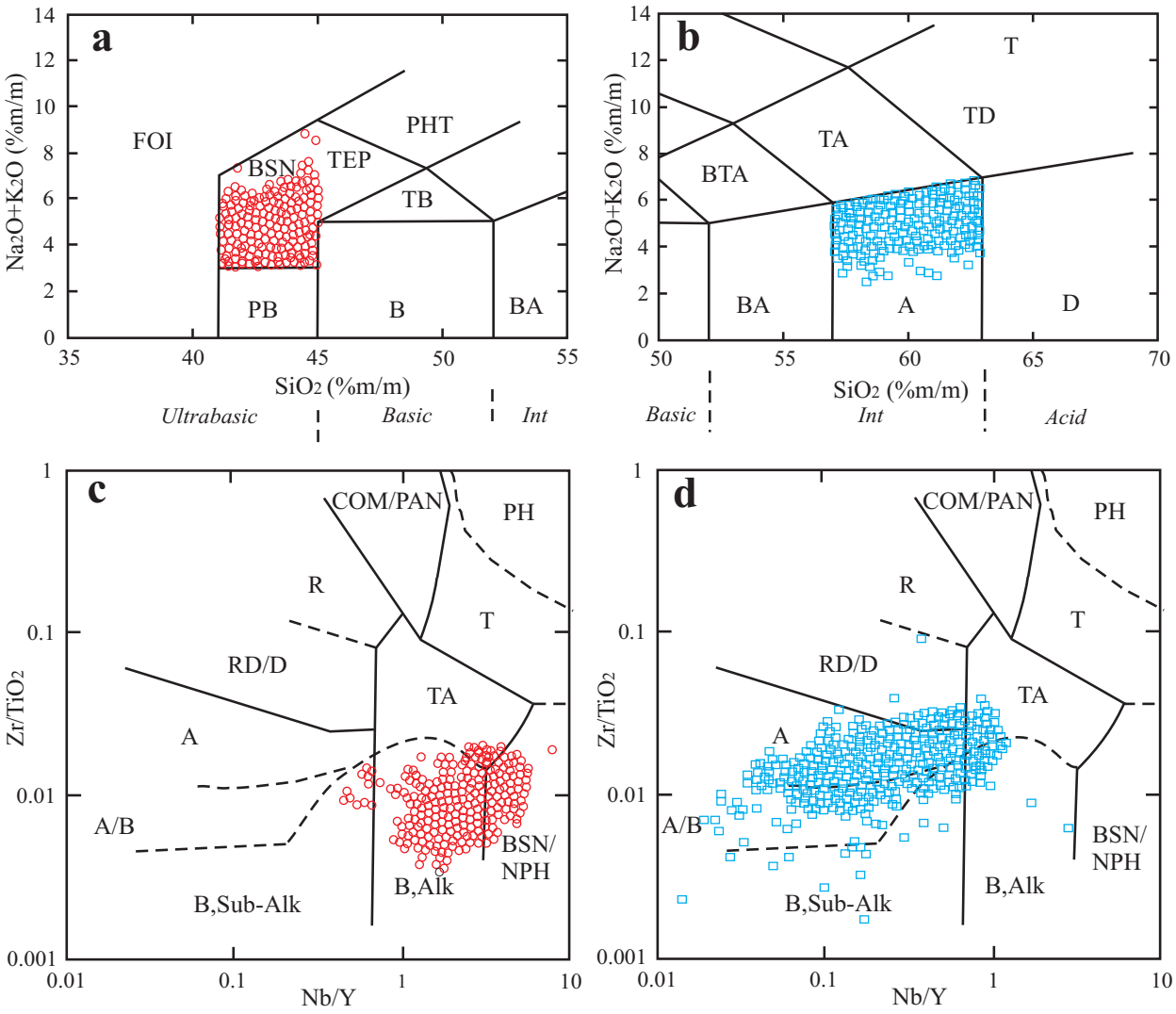

Figure 2. Statistical evaluation of the W&F diagram in reference to the TAS diagram using basanite and andesite rocks from our database. See Figure 1 for more explanation. **(a)** Basanite (541) samples according to the TAS diagram; **(b)** andesite (941) samples according to the TAS diagram; **(c)** the same basanite (541) samples of the TAS diagram plotted in the W&F diagram; and **(d)** the same andesite (941) samples of the TAS diagram plotted in the W&F diagram.

field had the same name as the initial IUGS rock name, it was said to represent correct classification or correct success rate (identified as ***italic boldface*** in Tables 1 & 2), whereas when the W&F field name differed from the IUGS, it was said to quantify misclassification (expressed as simple numbers – without highlighting– in Tables 1 & 2). All statistical information, including the number of samples and the calculated percentages, are included in Tables 1 and 2, respectively, for all data from four tectonic settings and those from three tectonic settings except island arc. For the IUGS rock names not present in the W&F diagram (second part of Tables 1 and 2), the highest percentage of the resulting rock W&F types was highlighted in *italics*.

We start the discussion with those rock types that exist in both the TAS and W&F classification. Then, those rock names absent from the W&F

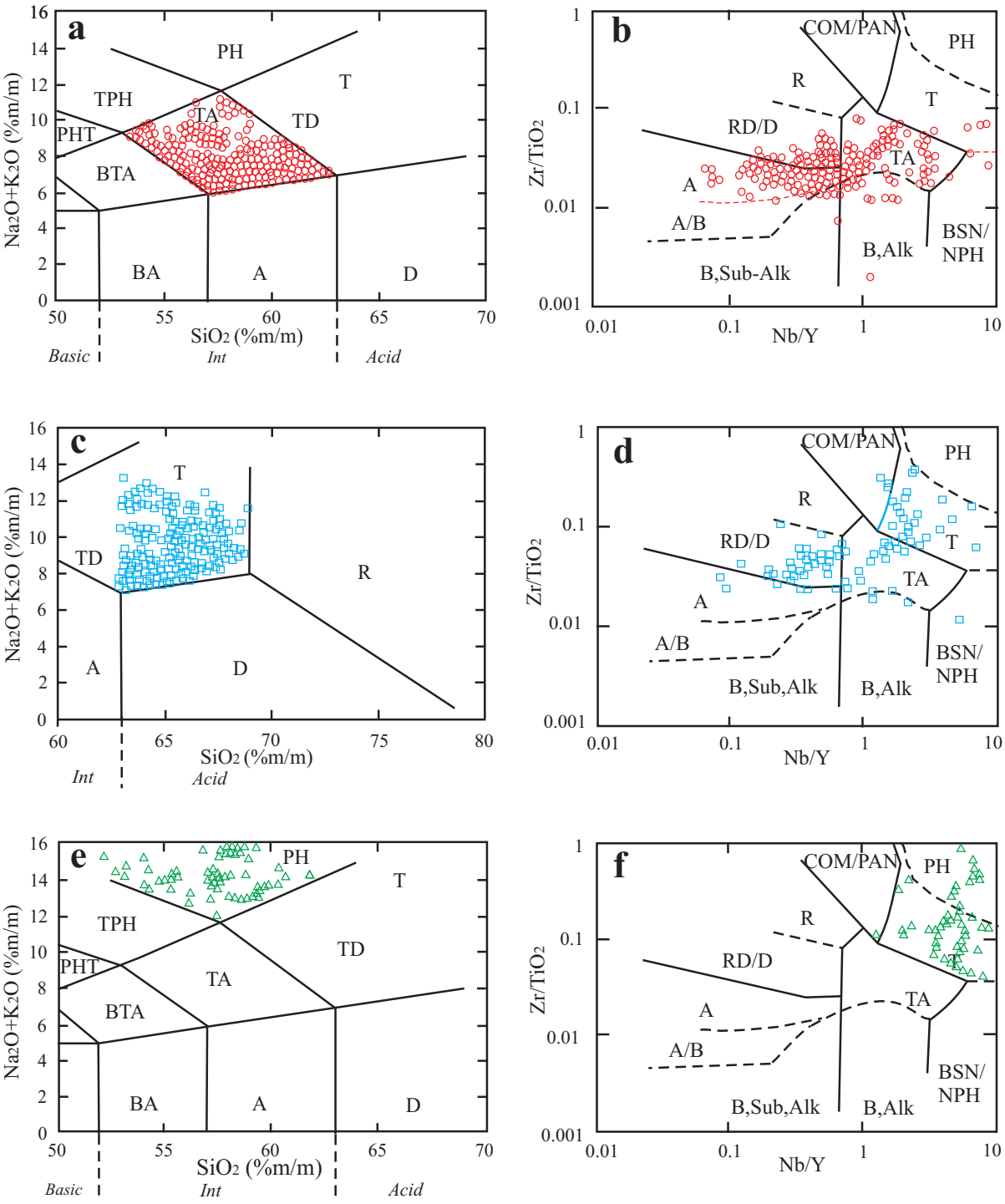

Figure 3. Statistical evaluation of the W&F diagram in reference to the TAS diagram using trachyandesite, trachyte and phonolite rocks from our database. See Figure 1 for more explanation. **(a)** Trachyandesite (222) samples according to the TAS diagram; **(b)** the same trachyandesite (222) samples of the TAS diagram plotted in the W&F diagram; **(c)** trachyte (81) samples according to the TAS diagram; **(d)** the same trachyte (81) samples of the TAS diagram plotted in the W&F diagram; **(e)** phonolite (49) samples according to the TAS diagram; and **(f)** the same phonolite (49) samples of the TAS diagram plotted in the W&F diagram.

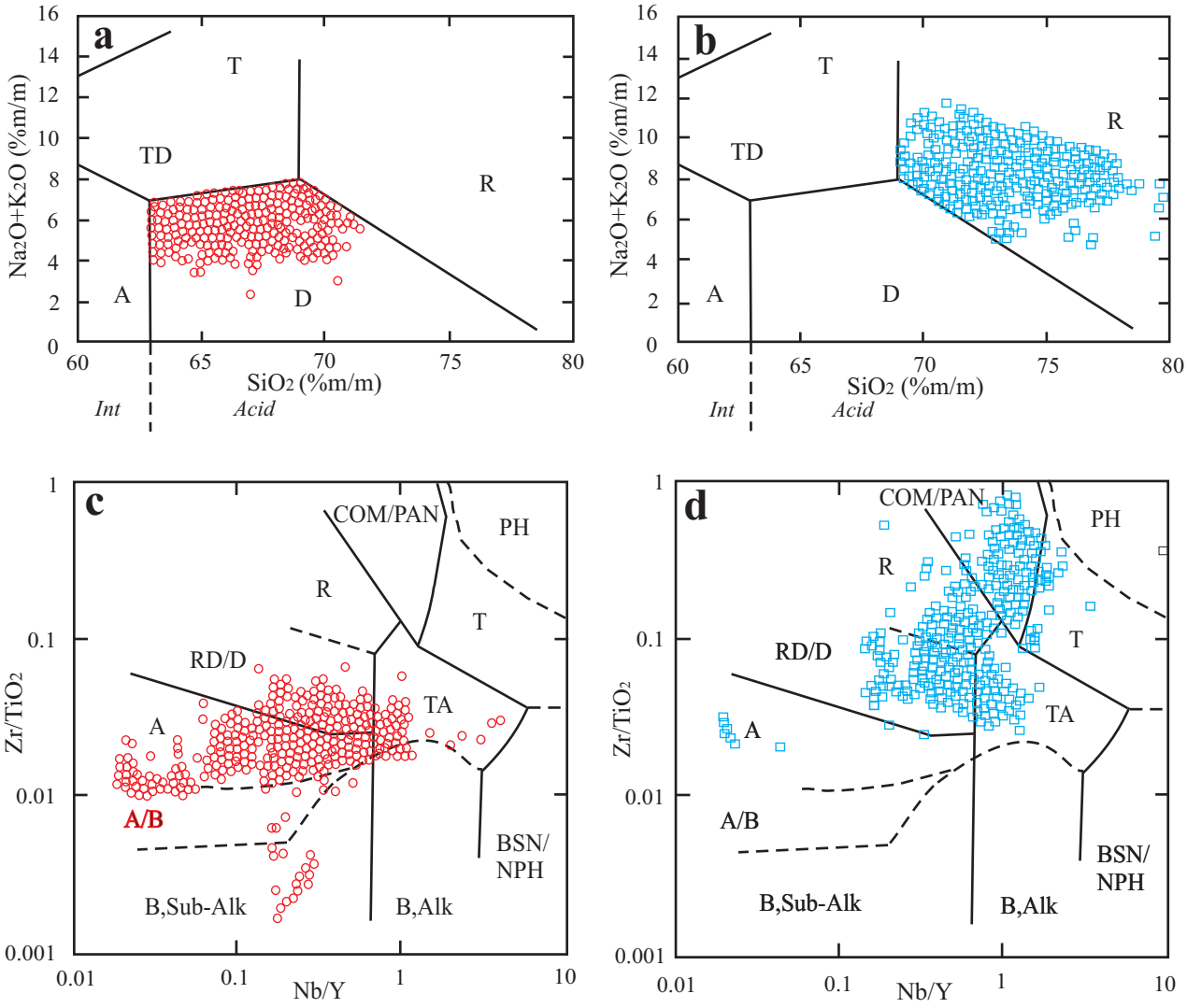

Figure 4. Statistical evaluation of the W&F diagram in reference to the TAS diagram using dacite and rhyolite rocks from our database. See Figure 1 for more explanation. **(a)** Dacite (524) samples according to the TAS diagram; **(b)** rhyolite (350) samples according to the TAS diagram; **(c)** the same dacite (524) samples of the TAS diagram plotted in the W&F diagram; and **(d)** the same rhyolite (350) samples of the TAS diagram plotted in the W&F diagram.

classification will be mentioned. The results of three tectonic settings –without arc rocks– will be discussed at the end of this subsection. In order to help the reader better understand our evaluation procedure, the results for alkali basalt and subalkaline basalt samples (Table 1) are presented in greater detail than the remaining rock types.

Our database used 650 samples of alkali basalt and 1200 of subalkaline basalt as classified from the IUGS nomenclature (the combination of TAS diagram and CIPW norm; Le Bas *et al.* 1986; Le Bas 2000; Le Maitre *et al.* 2002; Verma *et al.* 2002) – alkali basalt being a nepheline normative rock and subalkaline basalt a hypersthene normative rock, both of them with adjusted silica $(SiO_2)_{adj}$ between 45% and 52% and adjusted total alkalis $(Na_2O+K_2O)_{adj}$ up to 5%. The corresponding TAS diagrams showing these alkali basalt and subalkaline basalt samples are given in Figure 1a, b, respectively.

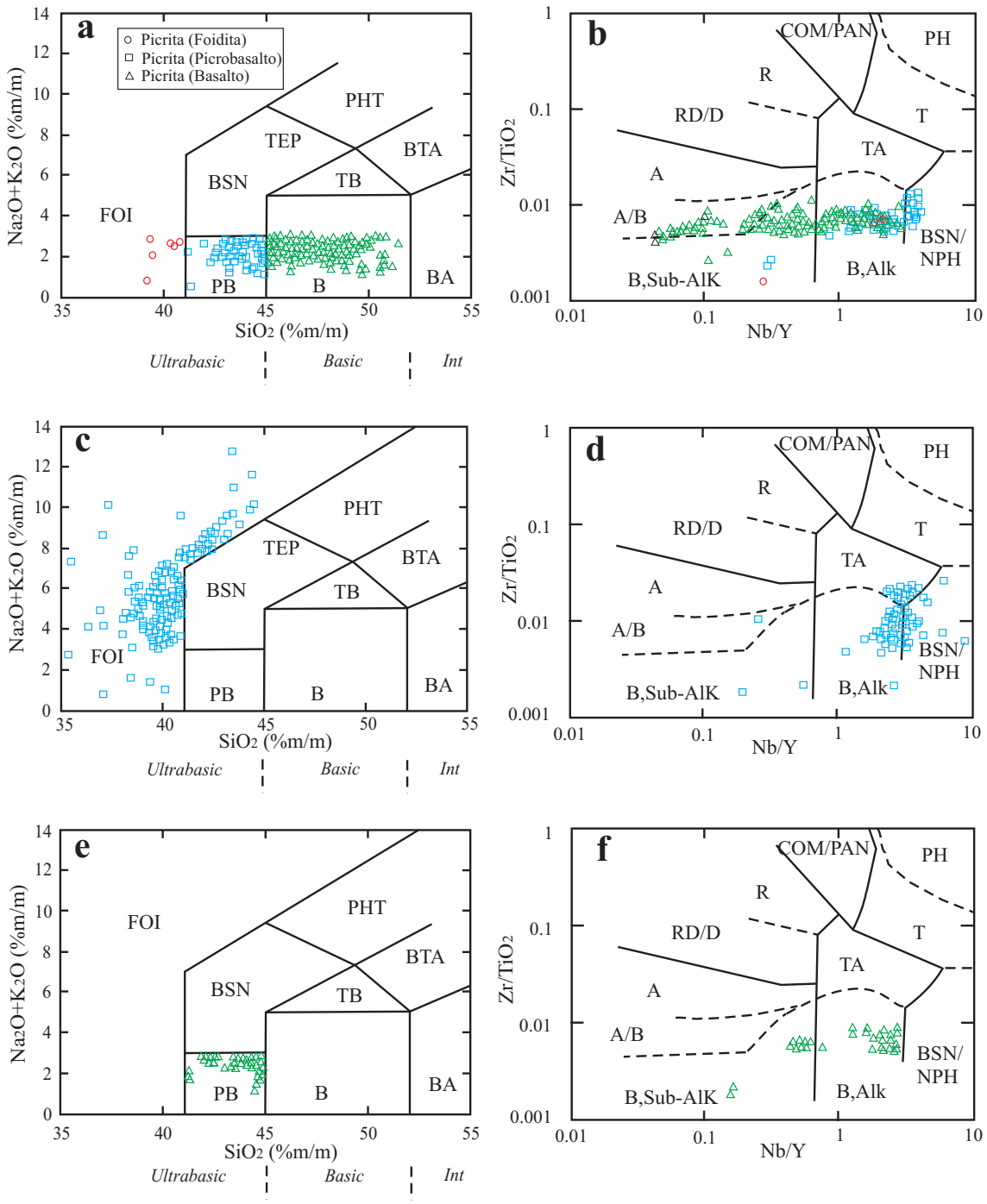

Figure 5. Statistical evaluation of the W&F diagram with reference to the TAS diagram using picrite (high-Mg rock, classified prior to the TAS diagram, although these rocks are plotted in TAS diagram for reference purposes only), foidite and picrobasalt rocks from our database. See Figure 1 for more explanation. **(a)** Picrite (total 151 samples; 45 samples similar to picrobasalt and 106 similar to alkali basalt) samples according to the TAS diagram; **(b)** the same picrite (151) samples of the TAS diagram plotted in the W&F diagram; **(c)** foidite (118) samples according to the TAS diagram; **(d)** the same foidite (118) samples of the TAS diagram plotted on the W&F diagram; **(e)** picrobasalt (30) samples according to the TAS diagram; and **(f)** the same picrobasalt (30) samples of the TAS diagram plotted on the W&F diagram.

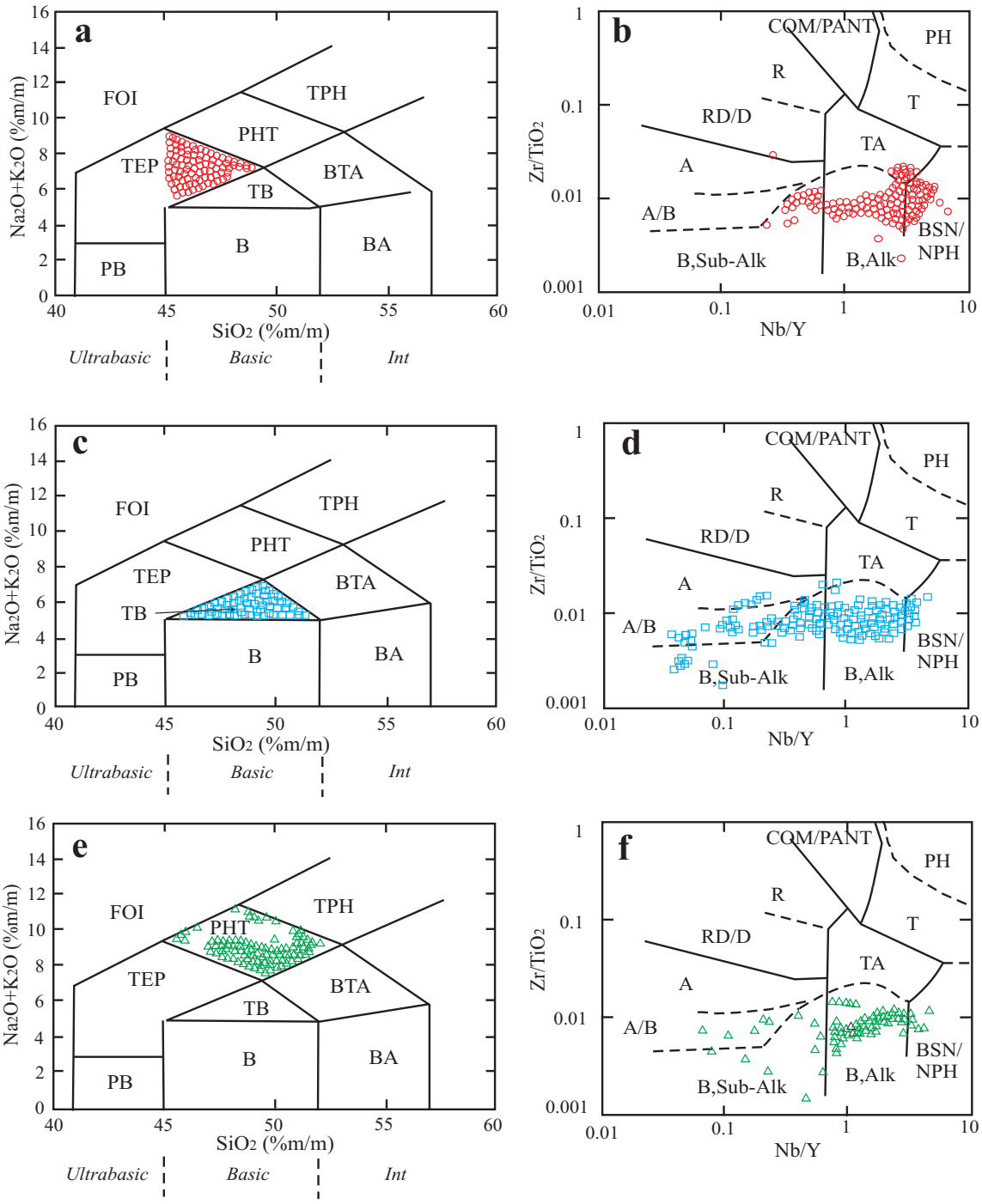

Figure 6. Statistical evaluation of the W&F diagram with reference to the TAS diagram, using tephrite, trachybasalt and phonotephrite rocks from our database. See Figure 1 for more explanation. **(a)** Tephrite (155) samples according to the TAS diagram; **(b)** the same tephrite (155) samples of the TAS diagram plotted on the W&F diagram; **(c)** trachybasalt (314) samples according to the TAS diagram; **(d)** the same trachybasalt (314) samples of the TAS diagram plotted on the W&F diagram; **(e)** phonotephrite (73) samples according to the TAS diagram; and **(f)** the same phonotephrite (73) samples of the TAS diagram plotted on the W&F diagram.

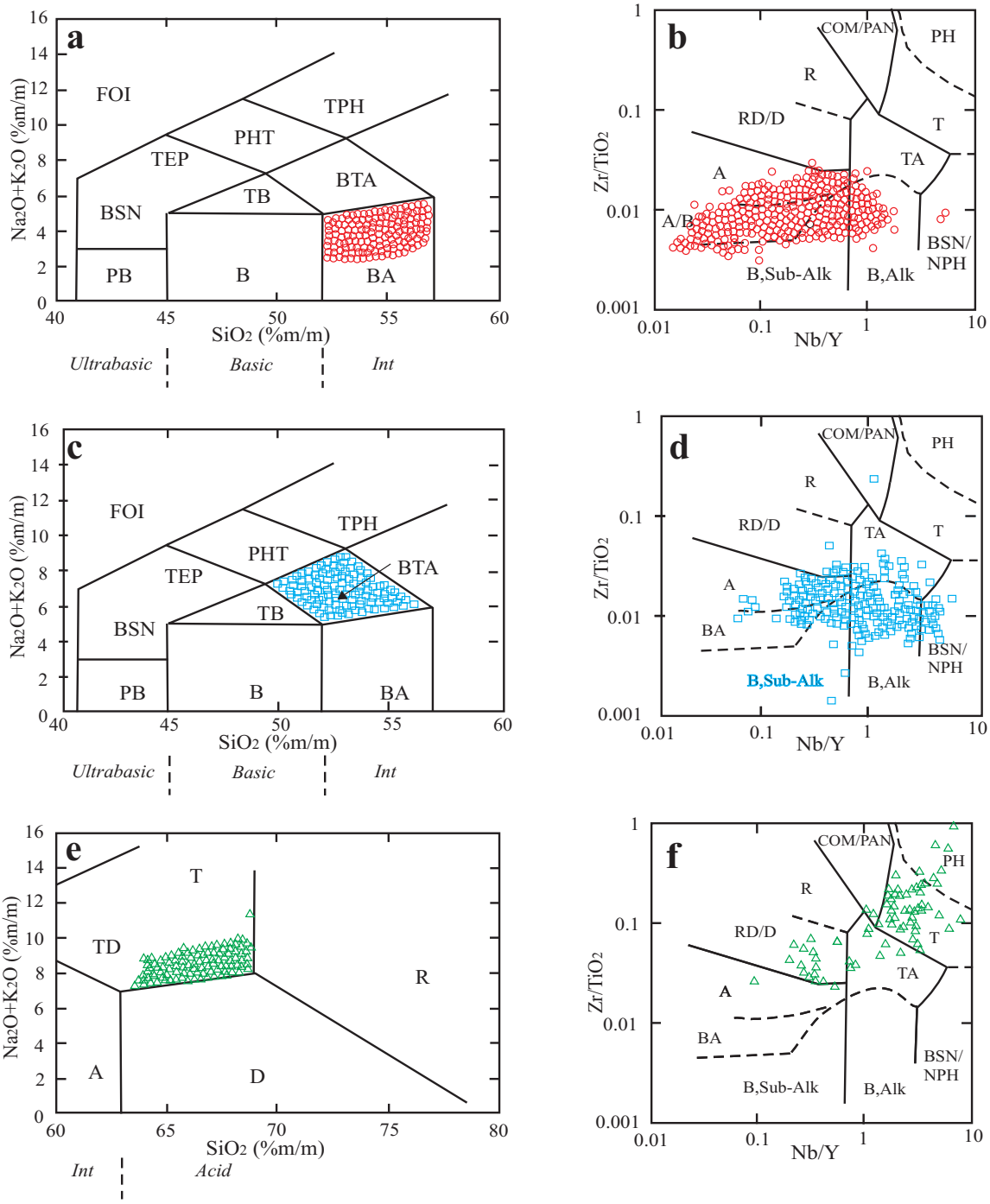

Figure 7. Statistical evaluation of the W&F diagram with reference to the TAS diagram, using basaltic andesite, basaltic trachyandesite and trachydacite rocks from our database. See Figure 1 for more explanation. **(a)** Basaltic andesite (1239) samples according to the TAS diagram; **(b)** the same basaltic andesite (1239) samples of the TAS diagram plotted on the W&F diagram; **(c)** basaltic trachyandesite (392) samples according to the TAS diagram; **(d)** the same basaltic trachyandesite (392) samples of the TAS diagram plotted on the W&F diagram; **(e)** trachydacite (69) samples according to the TAS diagram; and **(f)** the same trachydacite (69) samples of the TAS diagram plotted on the W&F diagram.

Table 1. Evaluation of the Nb/Y-Zr/TiO_2 diagram (Winchester & Floyd 1977; called here W&F diagram) as compared to the IUGS volcanic rock classification (TAS and CIPW norm; Le Bas *et al.* 1986; La Bas 2000; Le Maitre *et al.* 2002; Verma *et al.* 2002).

IUGS classification	Total number of samples (%)	Figure #	Number of classified samples (% of classified samples) according to Nb/Y-Zr/TiO_2 diagram (Winchester & Floyd 1977) W&F classification										
			Alkali-basalt	Sub-alkaline basalt	Basanite/ Nephelinite	Andesite/ basalt	Andesite	Trachyandesite	Trachyte	Phonolite	Comendite/ Pantellerite	Rhyodacite/ Dacite	Rhyolite
Alkali basalt	650 (100)	1a , 1c	***480 (73.8)***	81 (12.5)	20 (3.1)	59 (9.1)	9 (1.4)	1 (0.1)					
Subalkali basalt	1200 (100)	1b, 1d	313 (26.1)	***384 (32.0)***	9 (0.7)	470 (39.2)	23 (1.9)					1 (0.1)	
Basanite	541 (100)	2a , 2c	322 (59.5)	11 (2.0)	***161 (29.8)***				47 (8.7)				
Andesite	941 (100)	2b, 2d	40 (4.3)	34 (3.6)		87 (9.3)	***706 (75.0)***	35 (3.7)				39 (4.1)	
Trachyandesite	222 (100)	3a , 3d	16 (7.2)	7 (3.2)	3 (1.3)	2 (0.9)	85 (38.3)	***65 (29.3)***		4 (1.8)		40 (18.0)	
Trachyte	81 (100)	3b, 3e	2 (2.5)		1 (1.2)		6 (7.4)	15 (18.5)	***24 (29.6)***		3 (3.7)	30 (37.1)	
Phonolite	49 (100)	3c , 3f							11 (22)	***37 (76)***	1 (2)		
Dacite	524 (100)	4a, 4c	7 (1.4)	18 (3.4)		21 (4.0)	314 (59.9)	31 (5.9)				***133 (25.4)***	
Rhyolite	350 (100)	4b, 4d					9 (2.6)	57 (16.3)	1 (0.3)	22 (6.3)	109 (31.1)	94 (26.8)	***58 (16.6)***
Picrite (picrobasalt)	45 (100)	5a , 5b	*27 (60)*	2 (4)	16 (36)								
Picrite (alkali basalt)	106 (100)	5a , 5b	34 (32.1)	29 (27.3)		*43 (40.6)*							
Foidite	118 (100)	5c , 5d	*45 (38.1)*	2 (1.7)	37 (31.4)	1 (0.8)	33 (28.0)						
Picrobasalt	30 (100)	5e , 5f	*20 (67)*	10 (33)									
Tephrite	155 (100)	6a , 6b	*66 (42.6)*	20 (12.9)	50 (32.3)			18 (11.6)				1 (0.6)	
Trachybasalt	314 (100)	6c, 6d	*214 (68.2)*	49 (15.6)	12 (3.8)	31 (9.9)	7 (2.2)	1 (0.3)					
Phonotephrite	73 (100)	6e, 6f	*53 (72.6)*	9 (12.3)	6 (8.2)	5 (6.9)							
Basaltic andesite	1239 (100)	7a, 7b	98 (7.9)	262 (21.1)	2 (0.2)	*614 (49.6)*	259 (20.9)	3 (0.2)				1 (0.1)	
Basaltic trachyandesite	392 (100)	7c, 7d	*154 (39.3)*	62 (15.8)	20 (5.1)	27 (6.9)	94 (23.9)	26 (6.6)		1 (0.3)	1 (0.3)	7 (1.8)	
Trachydacite	69 (100)	7e, 7f					2 (2.9)	8 (11.6)	*36 (52.2)*	7 (10.1)	2 (2.9)	14 (20.3)	

Numbers in ***italic bold face*** are for the correct classification; numbers in *italic* show the rock type, in which most samples of rock types not included in W&F diagram were classified.

Table 2. Evaluation of Nb/Y-Zr/TiO_2 diagram (Winchester & Floyd 1977; called here W&F diagram) as compared to the IUGS volcanic rock classification (TAS and CIPW norm; Le Bas *et al.* 1986; La Bas 2000; Le Maitre *et al.* 2002; Verma *et al.* 2002), using rocks from all the tectonic settings except arc rocks (For more explanation, see Table 1).

IUGS classification	Total number of samples (%)	Figure #	Number of classified samples (% of classified samples) according to Nb/Y-Zr/TiO_2 diagram (Winchester & Floyd 1977) W&F classification										
			Alkali-basalt	Sub-alkaline basalt	Basanite/ Nephelinite	Andesite/ basalt	Andesite	Trachyandesite	Trachyte	Phonolite	Comendite/ Pantellerite	Rhyodacite/ Dacite	Rhyolite
Alkali basalt	556 (100)	1a, 1c	***470 (84.5)***	43 (7.7)	20 (3.6)	18 (3.2)	5 (0.9)						
Subalkali basalt	597 (100)	1b, 1d	291 (48.7)	***234 (39.2)***	9 (1.5)	60 (10.1)	2 (0.3)					1 (0.2)	
Basanite	536 (100)	2a, 2c	317 (59.1)	11 (2)	***161 (30)***			47 (8.8)					
Andesite	546 (100)	2b, 2d	36 (6.6)	16 (2.9)		22 (4)	***424 (77.6)***	24 (4.4)				24 (4.4)	
Trachyandesite	178 (100)	3a, 3b	10 (5.6)	4 (2.2)	3 (1.7)	2 (1.1)	50 (28.1)	***65 (36.5)***		4 (2.2)		40 (22.4)	
Trachyte	65 (100)	3c, 3d	2 (3)		1 (1.5)		3 (4.6)	15 (23.1)	***24 (36.9)***		3 (4.6)	17 (26.1)	
Phonolite	48 (100)	3e, 3f							36 (75)	***11 (22.9)***	1 (2)		
Dacite	272 (100)	4a, 4c	7 (2.5)	1 (0.4)		1 (0.4)	175 (64.3)	13 (4.7)				***75 (27.6)***	
Rhyolite	243 (100)	4b, 4d						21 (8.6)	22 (9)	1 (0.4)	108 (44.4)	46 (18.9)	***45 (18.5)***
Picrite (picrobasalt)	45 (100)	5a, 5b	*27 (60)*	2 (4.4)	16 (35.5)								
Picrite (alkali basalt)	80 (100)	5a, 5b	17 (21.2)	24 (30)		*39 (48.7)*							
Foidite	118 (100)	5c, 5d	*45 (38.1)*	2 (1.7)	37 (31.4)	1 (0.8)	33(28)						
Picrobasalt	29 (100)	5e, 5f	*19 (65.5)*	10 (34.5)									
Tephrite	155 (100)	6a, 6b	*66 (42.6)*	20 (12.9)	50 (32.3)			18 (11.6)				1 (0.6)	
Trachybasalt	247 (100)	6c, 6d	*176 (71.2)*	30 (12.1)	12 (4.8)	21 (8.5)	7 (2.8)	1 (0.4)					
Phonotephrite	66 (100)	6e, 6f	*48 (72.7)*	8 (12.1)	5 (7.5)	5 (7.5)							
Basaltic andesite	500 (100)	7a, 7b	85 (17)	192 (38.4)	1 (0.2)	*97 (19.4)*	122 (24.4)	3 (0.6)					
Basaltic trachyandesite	351 (100)	7c, 7d	*149 (42.4)*	57 (16.2)	18 (5.1)	23 (6.5)	70 (19.9)	26 (7.4)		1 (0.3)	1 (0.3)	6 (1.7)	
Trachydacite	65 (100)	7e, 7f					1 (1.5)	8 (12.3)	*36 (55.4)*	*7* (10.7)	2 (3)	11 (16.9)	

If these fresh rocks were to be classified correctly in the W&F diagram (Figure 1c, d; Nb/Y-Zr/TiO_2 diagram of Winchester & Floyd 1977), most of them (a high percentage) should be classified as alkali basalt and sub-alkaline basalt, respectively.

For alkali basalt, we observed (Table 1) that out of 650 (designated as 100%) samples from our databases, the correct classification according to the W&F diagram amounted to 480 (about 73.8%) samples. The misclassification of 170 (about 26.2%) samples (Table 1; Figure 1c) was as follows: 81 (about 12.5%) samples as sub-alkaline basalt; 59 (about 9.1%) as andesite/basalt; 20 (about 3.1%) as basanite/nephelinite; 9 (about 1.4%) as andesite; and 1 (about 0.1%) as trachyandesite. For subalkaline basalt, on the other hand, we observed that out of 1200 (100%) samples, only 384 (about 32.0%) were sub-alkaline basalt and most of them, i.e., the remaining 816 (about 68.0%) were misclassified (Figure 1d; Table 1). The misclassification for subalkaline basalt (Table 1) ranged as follows: 470 (about 39.2%) samples as of ambiguous type andesite/basalt; 313 (about 26.1%) as alkali-basalt; 23 (about 1.9%) as andesite; 9 (about 0.7%) as basanite/nephelinite; and 1 (about 0.1%) as rhyodacite/dacite. We also note that none of the alkali basalt samples was misclassified as trachyte, phonolite, comendite/pantellerite, rhyodacite/dacite, or rhyolite. Similarly, none of the subalkaline basalt was misclassified as trachyandesite, trachyte, phonolite, comendite/pantellerite, or rhyolite.

The results of basanite and andesite samples are plotted in Figure 2a–d. A total of 541 samples were separated as basanite from our database (Figure 2a; Table 1). The IUGS makes a distinction or sub-classification of basanite as basanite, melanephelinite and nephelinite, depending on the relative proportions of normative olivine, albite, and nepheline minerals (see Verma *et al.* 2002 for details). In the W&F diagram both basanite and nephelinite occupy exactly the same field (Figure 2c). Therefore, we did not make any further distinction of IUGS classification of basanite. Most of these 541 (100%) samples of basanite were misclassified by the W&F scheme, with 322 (59.5%) of them being misclassified as alkali-basalt (Figure 2c; Table 1). Only 161 (29.8%) samples were correctly classified as basanite/nephelinite. The remaining basanite samples were misclassified as trachyte (47 samples) and sub-alkaline basalt (11 samples). Our database included 941 andesite samples according to the IUGS classification scheme (Figure 2b), which were plotted in Figure 2d of the W&F diagram. Of these, 706 (75.0%) samples were correctly identified as andesite (Table 1) followed by 87 (9.3%) as ambiguous andesite/basalt. The remaining misclassification consisted of 40 (4.3%) samples as alkali-basalt, 39 (4.1%) as rhyodacite/dacite, 35 (3.7%) as trachyandesite, and 34 (3.6%) as sub-alkaline basalt.

Evaluation of the W&F diagram for trachyandesite, trachyte and phonolite is presented in Figure 3a–f and summarised in Table 1. Our test of 222 trachyandesite samples from our database (Figure 3a) revealed that this type of rock was very poorly classified in the W&F diagram (Figure 3b), with only 65 (29.3%) samples corrected classified as such (Table 1). Most samples (85 representing 38.3%) were misclassified as andesite (Table 1). This misclassification was followed by 40 (18.0%) samples as ambiguous types (rhyodacite/dacite) and 16 (7.2%) samples as alkali-basalt (Table 1), with the remaining (16) samples as other rock types. Evaluation of the W&F diagram using 81 trachyte samples (Figure 3c) revealed that only 24 (about 29.6%) samples were correctly classified as trachyte, with the remaining mostly misclassified as rhyodacite/dacite and trachyandesite (30 samples–37.1% and 15 samples–18.5%, respectively; Figure 3d; Table 1). Only 49 samples were classified as phonolite in our database (Figure 3e). According to W&F, the correct classification for them amounted to 37 (about 76%) as phonolite, with most (11) remaining samples (22%) being misclassified as trachyte (Figure 3f; Table 1).

Finally, our database had a fairly large number of samples of dacite and rhyolite (524 and 350, respectively) as determined by the IUGS classification (Table 1; Figure 4a, b). Their correct classification by the W&F diagram was very poor (Figure 4c, d), with only 133 (25.4%) samples as rhyodacite/dacite and 58 (16.6%) as rhyolite, respectively. The majority of samples, therefore, were misclassified (Table 1). Dacite samples were misclassified mostly as andesite (314 samples; 59.9%)

and rhyolite samples as comendite/pantellerite (109 samples; 31.1%) and rhyodacite/dacite (94 samples; 26.8%).

The remaining rock names of the IUGS classification were not included in the W&F classification. These are briefly treated, approximately from high-Mg varieties and ultrabasic to acid types. The lower part of Table 1 also provides statistical information on the W&F classification of these samples. The rock names comendite and pantellerite used by Winchester & Floyd (1977) were not incorporated by the IUGS scheme (Le Bas *et al.* 1986; Le Bas 2000; Le Maitre *et al.* 2002) and, therefore, could not be evaluated.

For high-Mg picrite magmas, our database provided 157 samples. Note that picrites are not classified by the TAS diagram (Le Bas 2000). However, to continue to explore the relationship of the TAS diagram with the W&F diagram, we made an artificial distinction of picrites according to the TAS field in which they would plot (Figure 5a). Thus, these 157 samples of picrites were sub-divided as: 6 samples only as picrite (foidite); 45 as picrite (picrobasalt); and 106 as picrite (alkali basalt). The W&F classification of these six picrite (foidite) samples was not considered statistically significant. The 45 picrite samples of picrobasalt type were classified (Table 1; Figure 5b) as alkali-basalt (27 samples), basanite/nephelinite (16 samples) and sub-alkaline basalt (2 samples). The 106 picrite samples of alkali basalt type, on the other hand, were classified as andesite/basalt (43 samples), alkali-basalt (34 samples) and sub-alkaline basalt (29 samples). Our databases included 118 samples (Figure 5c) of foidite, an ultrabasic rock. When these samples were plotted in the W&F diagram (Figure 5d), we observed that 45 samples (about 38.1%) were classified as alkali-basalt, 37 (31.4%) as basanite/nephelinite, 33 (28.0%) as andesite, 2 (1.7%) as sub-alkaline basalt, and 1 (0.8%) as andesite/basalt. Only 30 samples of picrobasalt were compiled in our database (Figure 5e), which were classified as alkali-basalt and sub-alkaline basalt in the W&F diagram (20 and 10 respectively; Figure 5f).

For tephrite (155 samples), trachybasalt (314 samples), and phonotephrite (73 samples), the results summarised in Figure 6a–f and Table 1 showed that these rock types were mostly classified by the W&F diagram as alkali-basalt (66, 214, and 53 samples, respectively). Additionally, for these three rock types a significant number of samples (20, 49, and 9, respectively) were recognised as subalkaline basalt (Table 1). For tephrite samples, basanite/nephelinite also represented an important W&F classification (50 samples; 32.3%). A significant number of tephrite samples (18; 11.6%) were classified as trachyandesite in the W&F scheme.

Finally, we present the remaining three important rock types (basaltic andesite, basaltic trachyandesite, and trachydacite) according to the IUGS classification (Table 1; Figure 7a, c, e), but not included as such in the W&F diagram (Figure 7b, d, f). For basaltic andesite a very large number of samples (1239) were present in our database (Figure 7a). These were classified (Figure 7b) mainly as andesite/basalt (614 samples; 49.6%), sub-alkaline basalt (262 samples; 21.1%), and andesite (259 samples; 20.9%). Similarly, Figure 7c, d and Table 1 show that 392 samples of basaltic trachyandesite were classified mainly as alkali-basalt (154 samples; 39.3%), andesite (94 samples; 23.9%), and sub-alkaline basalt (62 samples; 15.8%). Our final rock type trachydacite was represented by 69 samples (Figure 7e), which were classified mainly as trachyte and rhyodacite/dacite (36 samples–52.2% and 14 samples–20.3%, respectively; Figure 7f; Table 1).

In summary, the correct classification by the W&F diagram (Winchester & Floyd 1977) ranged from very low values of about 16.6% to reasonably high values of 76%. Alkali basalt, andesite and phonolite were best classified as such (about 73.8–76%). The classification for subalkaline basalt, basanite, trachyandesite, dacite, and rhyolite (with 16.6–32.0%) was simply not acceptable. The remaining nine rock types included in the IUGS classification (Figures 5–7) also did not provide any one coherent rock name in the W&F scheme; the highest percentages ranged from 38.1% to 72.6%. Therefore, the wide use of this Nb/Y-Zr/TiO_2 diagram currently in practice is not particularly justified.

In order to obtain a totally unbiased evaluation of the W&F diagram, which is not particularly

recommended for classifying arc rocks, we prepared a selected database by excluding all arc rocks and once again evaluated this diagram. The results are summarised in Table 2. To limit the space of this paper, no new diagrams are presented, as all these samples are already included in Figures 1–7). As expected, the total number of samples of a given rock type generally decreased in Table 2 as compared to Table 1, and this decrease was more pronounced for sub-alkaline varieties than for alkaline types. In fact, exactly the same number of samples of picrite and foidite remained in Table 2 as in Table 1.

For alkali basalt samples, the correct classification by the W&F diagram increased from 73.8% to 84.5% (compare Tables 1 & 2), but for subalkaline basalt it still remained unacceptably low (39.2%; Table 2). Basanite, trachyandesite, trachyte, and phonolite were also not satisfactorily classified by the W&F diagram (correct classification of only about 30%, 36.5%, 36.9%, and 22.9%, respectively). Although andesite rock samples were fairly well classified as such (77.6%), neither dacite nor rhyolite samples had acceptable correct classifications (27.6% classified as ambiguous rhyodacite/dacite and 18.5% as rhyolite, respectively; Table 2). For rock types not included in the W&F classification (the second part of Table 2), the classification results remained practically the same as in Table 1.

From this work, therefore, an urgent need of an improved classification scheme for altered rocks is clearly established.

New Classification Diagram

Recently Hastie *et al.* (2007) recognised from an altogether different approach (analysis of the chemical effects of alteration) that there is need for 'a reliable way to classify rocks from the geological record'. They stated that none of the frequently used SiO_2-K_2O (Peccerillo & Taylor 1976) and the IUGS recommended TAS (Le Bas *et al.* 1986) diagrams are appropriate for this purpose. They also argued that although Winchester & Floyd (1977) developed immobile element proxies for the TAS diagram, the need still existed for proxies of the SiO_2-K_2O diagram. Hastie *et al.* (2007) proposed the use of two proxy elements –Co for SiO_2 and Th for K_2O– in a new Co-Th bivariate diagram. Their contention that the W&F diagram is appropriate to replace the TAS diagram has already been shown to be deficient in the present work (see above).

We now attempt to evaluate the new Co-Th diagram for classification purposes (Hastie *et al.* 2007). The same database as the one used for the evaluation of the W&F diagram was employed, with the addition of the Andes and the Mexican Volcanic Belt. We decided not to use the SiO_2-K_2O plot for processing our database because we wanted to strictly follow the IUGS recommendations for rock names (Le Bas *et al.* 1986; Le Bas 2000), in which the SiO_2-K_2O scheme (e.g., Peccerillo & Taylor 1976) was not included. Further, an evaluation of Co-Th diagram in terms of SiO_2-K_2O scheme was already provided by the original authors (Hastie *et al.* 2007) who concluded that success rates ranged only up to about 80% and, therefore, were not particularly high.

In this context, the subdivision of rock types in the Co-Th diagram is rather poor (Hastie *et al.* 2007). Actually only three independent regions for rock names were proposed in this diagram: basalt; an overlap region of basaltic andesite with andesite (referred to in this work as 'basaltic andesite/andesite'); and an overlap region of dacite with rhyolite that also includes latite and trachyte ('dacite/rhyolite/latite/trachyte'). Each of these three regions is further subdivided into tholeiitic, calc-alkaline, and high-K_2O/shoshonitic. The correspondence of this three-fold subdivision of alkali-enrichment with the IUGS classification is difficult to establish. In the later scheme, only two-fold subdivision –subalkaline and alkali– may be implicitly imagined for basalt. Certainly, there are many rock names depending on the contents of total alkalis at any given silica level. For example, at the same silica level the IUGS rock names can vary from basaltic andesite, basaltic trachyandesite, tephrite to phonolite, or from andesite, trachyandesite to phonolite (Le Bas *et al.* 1986; Verma *et al.* 2002). For basaltic magmas, we could have arbitrarily used the adjective subalkaline for both tholeiitic and calc-alkaline divisions and alkali for high-K_2O/shoshonite. However, in our evaluation of the Co-Th diagram we decided not to enter into this oversimplification or assumptions regarding the

IUGS nomenclature. Instead, separate identities of the three-fold subdivision of the Co-Th diagram were maintained.

Nevertheless, some clarification must be made for the correct classification (also called success rate) and consequently for the misclassification. For example, when a single basic rock type, such as basalt (IUGS nomenclature), was used for evaluation and if the rock name resulting from the Co-Th diagram for a basalt sample was not basalt, this particular sample represented an obvious misclassification. Thus, for a group of samples of a given rock type it was easier to determine the 'obvious misclassification' or also called here the 'minimum misclassification'. The latter term will be used and highlighted in our following presentation. We will not explicitly refer to correct classification or success rate, because it will be more difficult to determine for the Co-Th diagram of Hastie *et al.* (2007) than for the old W&F diagram. In the former, the rock names are limited to only three separate fields.

Hastie *et al.* (2007) mentioned that their diagram is especially useful for the classification of arc rocks. Therefore, we maintained the identity of the tectonic setting or volcanic provinces used in this evaluation. These were: island arc, continental arc of the Andes, MVB, continental rift, and for some rock types additionally, ocean island. The results of our evaluation are presented in Figures 8–10 and summarised in Table 3. The 'minimum misclassification' is shown in **boldface** for rock names common to both classifications (IUGS and Co-Th diagram), or in *italics* for rock names not included in the IUGS classification (Table 3). Note especially that this highlighting is the reverse to that used for the W&F classification (Tables 1 & 2), in which the correct classification was shown in ***italic*** **boldface**.

For subalkaline basalt from island arcs (237 samples with Co and Th data compiled in our database; Figure 8a), the minimum misclassification amounted to 44 samples (18.6%) as basaltic andesite/andesite (Figure 8b; Table 3). A total of 193 remaining samples were, therefore, identified as the three varieties of basalt (see the columns of Thol., CA, and SHO in Table 3). The eight shoshonite samples could also be considered as obvious misclassification, but we decided not to discuss such finer details. For subalkaline basalt (47 samples) from the Andes, 4 samples (about 8%) were obviously misclassified as basaltic andesite or andesite. For subalkaline basalt samples from the MVB and continental rift settings, no obvious misclassification was observed. This does not mean, however, that the complement was the correct classification or success rate, we simply cannot clearly define it, as discussed earlier.

The minimum misclassification of alkali basalt samples (Figure 8c) was much less, with only a few samples misclassified as basaltic andesite/andesite (Figure 8d; Table 3).

For the total of 206 samples of basaltic andesite from island arc setting (Figure 9a), a larger number of them (99 samples amounting to about 48.1%) represented the minimum misclassification: 93 samples (45.2%) as basalt. and 6 samples (2.9%) as dacite/rhyolite/ latite/trachyte (Figure 9b; Table 3). An even greater extent of minimum misclassification was observed for these rock types from the Andes (Figure 9b), because 87 samples out of 138 (63.1%) were misclassified as basalt and only the remaining 51 samples (36.9%) plotted correctly as basaltic andesite/andesite (Table 3). As for the Andes, the minimum misclassification for basaltic andesite from the MVB was also significant –about 50.4% (Table 3). For continental rifts, misclassification was extremely high (about 93%), with 37 out of 40 samples misclassified as basalt (Figure 9b).

Andesite (Figure 9c) can only be classified ambiguously as basaltic andesite/andesite (Figure 9d; Table 3). The minimum misclassification of andesite samples from island arcs, the Andes, and MVB as basalt was, respectively, about 12.8%, 23.7%, and 14.6% dacite/rhyolite/latite/trachyte (Figure 9d; Table 3).

Dacite, trachyte, trachydacite and rhyolite (Figure 9e) were considered together because they could only be classified as a group by the Co-Th diagram (Figure 9f). Such rock samples from island arc and the Andes showed 25.3% and 29.5% minimum misclassification, respectively (Table 3). Similarly, the MVB and continental rift setting had values of 30.1% and 24.0%, respectively.

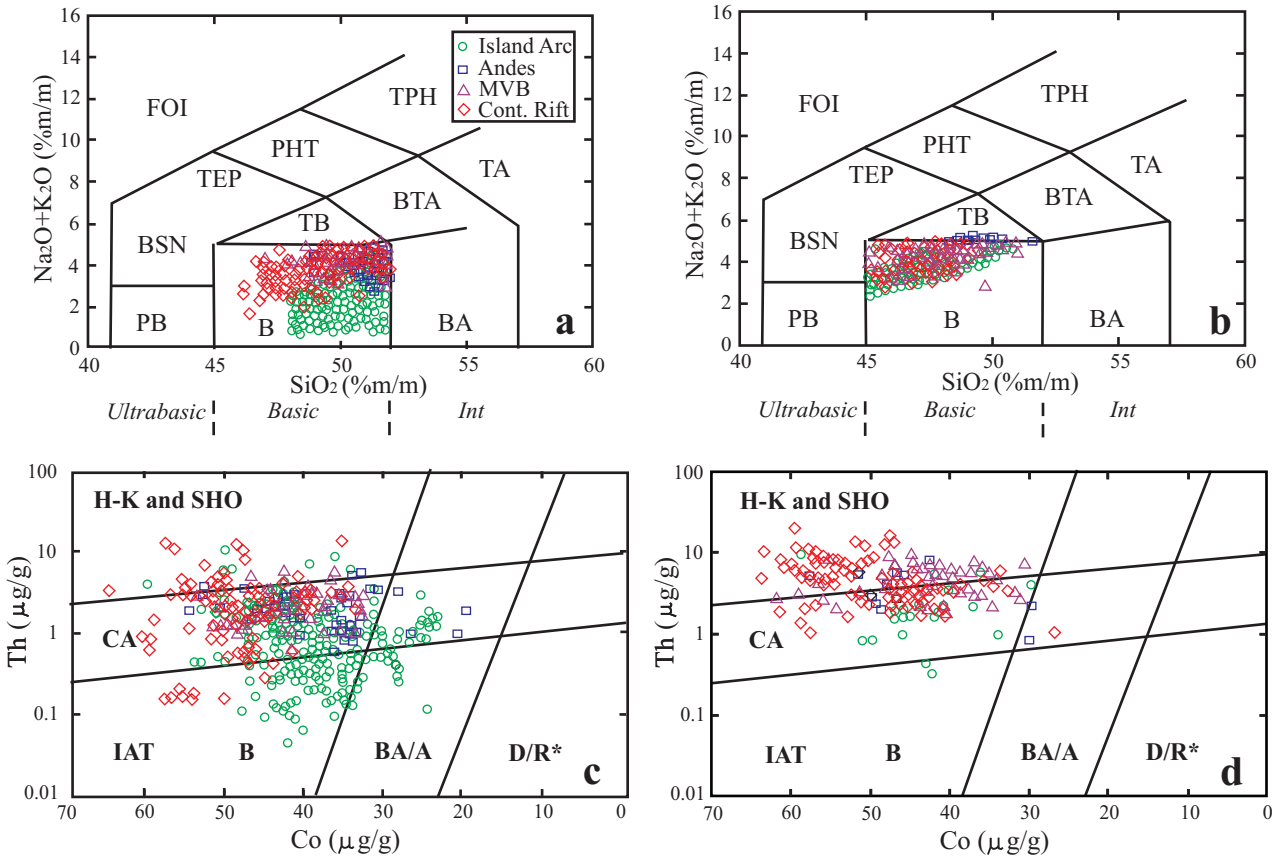

Figure 8. Statistical evaluation of the Co-Th diagram of Hastie *et al.* (2007) with reference to the TAS (total alkalis *versus* silica) diagram (Le Bas *et al.* 1986; Verma *et al.* 2002) of the IUGS classification scheme, using basaltic rocks from our database. Note that the separate identity of tectonic settings was maintained in this and later diagrams. See Figure 1 for more explanation on the TAS diagram. The rock type abbreviations in the Co-Th diagram are: B– basalt; BA/A– basaltic andesite/andesite; D/R*– dacite/rhyolite/latite/trachyte; IAT– island arc tholeiite; CA– calc-alkaline; and H-K and SHO– high-K and shoshonite (see also Table 3). The same symbols are used in both the Co-Th diagram and the corresponding TAS diagram. Furthermore, they are explained as inset in (a). **(a)** Subalkaline basalt (437 samples; 237 from island arcs, 47 from the Andes, 61 from the Mexican Volcanic Belt–MVB, and 92 from continental rifts) according to the TAS diagram; **(b)** alkali basalt (167 samples; 22 from island arcs, 12 from the Andes, 48 from the MVB, and 85 from continental rifts) according to the TAS diagram; **(c)** the same subalkaline basalt (437) samples of the TAS diagram plotted on the Co-Th diagram; and **(d)** the same alkali basalt (167) samples of the TAS diagram plotted on the Co-Th diagram.

The remaining results synthesised in Table 3 are for rock names (from the IUGS nomenclature) that were excluded from the Co-Th diagram of Hastie *et al.* (2007). These rocks (Figure 10a–f) are mostly more alkalic than the earlier rocks already evaluated and presented in the first part of Table 3. In this second part of Table 3, combined rock types are arranged in the following order: ultrabasic (two groups; Figure 10a, b), basic (four groups; Figure 10c, d), and intermediate to acid (five groups; Figure 10e, f).

As expected, ultrabasic magmas are rather scarce in island arcs (no arc samples in Figure 10a; Table 3) and alkali-rich rocks, such as basaltic trachyandesite, trachybasalt, trachyte and trachyandesite, are much less abundant in island arc settings than in other tectonic areas, including the MVB and continental arc of the Andes (Figure 10c, e; Table 3). Three out of

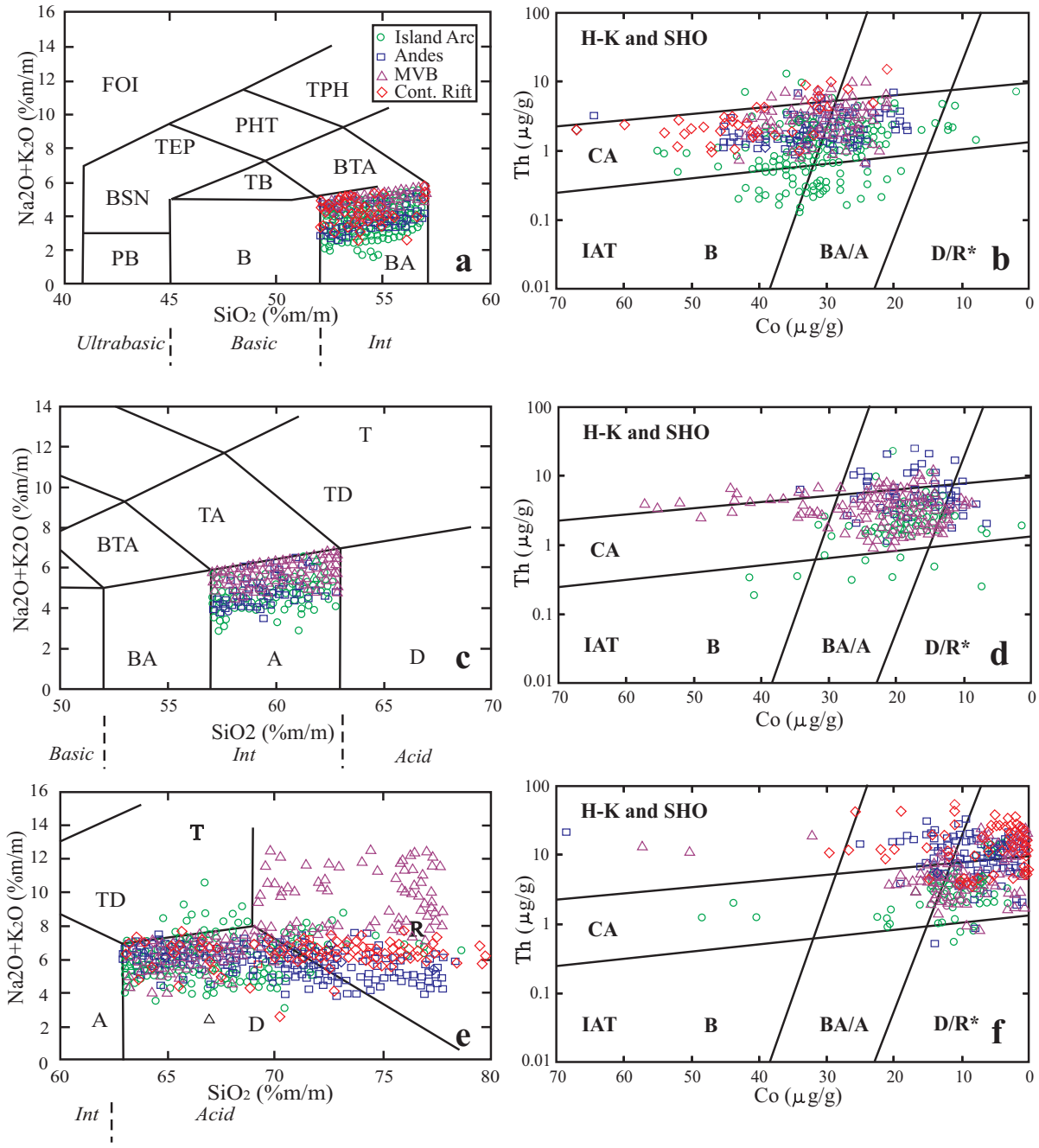

Figure 9. Statistical evaluation of the Co-Th diagram of Hastie *et al.* (2007) with reference to the TAS (total alkalis *versus* silica) diagram (Le Bas *et al.* 1986; Verma *et al.* 2002), using basaltic andesite, andesite, dacite, trachyte, trachydacite and rhyolite rocks from our database. See Figures 1 and 8 and Table 3 for more explanation. **(a)** Basaltic andesite (513 samples; 206 from island arcs, 138 from the Andes, 129 from the MVB, and 40 from continental rifts) according to the TAS diagram; **(b)** the same basaltic andesite (513) samples of the TAS diagram plotted on the Co-Th diagram; **(c)** andesite (456 samples; 109 from island arcs, 59 from the Andes, and 288 from the MVB) according to the TAS diagram; **(d)** the same andesite (456) samples of the TAS diagram plotted on the Co–Th diagram; **(e)** diverse acid rock types (436 samples; 83 from island arcs, 112 from the Andes, 166 from the MVB, and 75 from continental rifts) according to the TAS diagram; and **(f)** the same (436) samples of the TAS diagram plotted on the Co-Th diagram.

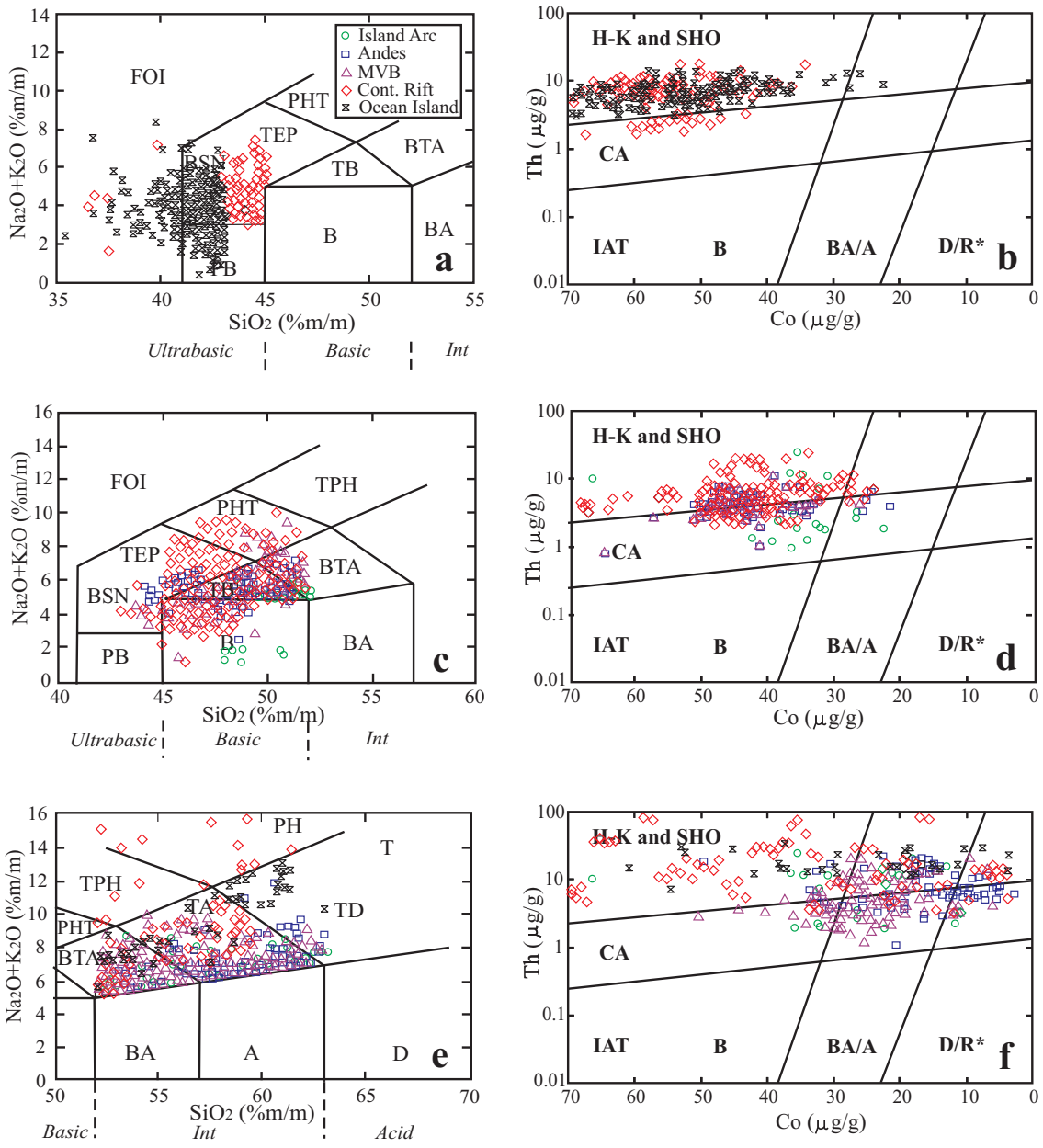

Figure 10. Statistical evaluation of the Co-Th diagram of Hastie *et al.* (2007) with reference to the TAS (total alkalis *versus* silica) diagram (Le Bas *et al.* 1986; Verma *et al.* 2002), using diverse rocks (other than those used in Figures 8 & 9) from our database. See Figures 1 and 8 and Table 3 for more explanation. **(a)** Different combinations of rock types (see Table 3 for abbreviations; 86 from continental rifts and 180 from ocean islands) according to the TAS diagram; **(b)** the same samples of the TAS diagram (a) plotted on the Co-Th diagram; **(c)** different combinations of rock types (see Table 3 for abbreviations; 19 samples from island arcs, 51 from the Andes, 45 from the MVB, and 134 from continental rifts) according to the TAS diagram; **(d)** the same samples of the TAS diagram (c) plotted on the Co-Th diagram; **(e)** different combinations of rock types (see Table 3 for abbreviations; 18 from island arcs, 70 from the Andes, 94 from the MVB, 67 from continental rifts, and 29 from ocean islands) samples according to the TAS diagram; and **(f)** the same samples of the TAS diagram (e) plotted on the Co-Th diagram.

Table 3. Evaluation of the Co-Th diagram (Hastie *et al.* 2007) for the classification of fresh volcanic rocks from different tectonic settings, as compared to the IUGS volcanic rock classification (TAS and CIPW norm; Le Bas *et al.* 1986; La Bas 2000; Le Maitre *et al.* 2002; Verma *et al.* 2002).

IUGS classification	Tectonic Setting	No. of Samples (%)	Figure #	B			BA/A			D/R*		
				Thol.	CA	SHO	Thol.	CA	SHO	Thol.	CA	SHO
B,subalk	Island arc	237 (100)	8a, 8c	64 (27.0)	121 (51.0)	8 (3.4)	**19 (8.0)**	**25 (10.6)**				
B,subalk	The Andes	47 (100)	8a, 8c		39 (84)	4 (8)		**4 (8)**				
B,subalk	MVB	61 (100)	8a, 8c		56 (91.8)	5 (8.2)						
B,subalk	Continental rift	92 (100)	8a, 8c	8 (8.7)	63 (68.5)	21 (22.8)						
B,alk	Island arc	22 (100)	8b, 8d	2 (9)	17 (77)	3 (14)						
B,alk	The Andes	12	8b, 8d		4	6		**2**				
B,alk	MVB	48 (100)	8b, 8d	20 (42)		28 (58)						
B,alk	Continental rift	85 (100)	8b, 8d		38 (44.7)	46 (54.1)		**1 (1.2)**				
BA	Island arc	206 (100)	9a, 9b	**19 (9.2)**	**70 (34.0)**	**4 (2.0)**	25 (12.1)	82 (39.8)			**6 (2.9)**	
BA	The Andes	138 (100)	9a, 9b		**83 (60.2)**	**4 (2.9)**	1 (0.7)	49 (35.5)	1 (0.7)			
BA	MVB	129 (100)	9a, 9b		**57 (44.2)**	**8 (6.2)**	1 (0.8)	58 (45.0)	5 (3.8)			
BA	Continental rift	40 (100)	9a, 9b	**9 (23)**	**28 (70)**		2 (5)	1 (2)				
A	Island arc	109 (100)	9c, 9d	**3 (2.8)**	**2 (1.8)**		4 (3.7)	88 (80.7)	3 (2.8)	**2 (1.8)**	**7 (6.4)**	
A	The Andes	59 (100)	9c, 9d			**1 (1.7)**		26 (44.1)	19 (32.2)		**12 (20.3)**	**1 (1.7)**
A	MVB	288 (100)	9c, 9d		**9 (3.1)**	**12 (4.2)**		230 (79.9)	16 (5.5)		**21 (7.3)**	
D+T+TD+R	Island arc	83 (100)	9e, 9f		**3 (3.6)**			**18 (21.7)**		4 (4.8)	47 (56.6)	11 (13.3)
D+T+TD+R	The Andes	112 (100)	9e, 9f			**1 (0.9)**		**5 (4.5)**	**27 (24.1)**	2 (1.8)	20 (17.8)	57 (50.9)
D+T+R	MVB	166 (100)	9e, 9f			**3 (1.8)**		**41 (24.7)**	**6 (3.6)**	2 (1.2)	75 (45.2)	39 (23.5)
D+T+TD+R	Continental rift	75 (100)	9e, 9f			**2 (2.6)**		**2 (2.6)**	**14 (18.8)**		18 (24.0)	39 (52.0)
BSN+FOI+PIC+TEP	Continental rift	86 (100)	10a, 10b		22 (25.6)	64 (74.4)						
BSN+FOI+PB+PIC+TEP	Ocean Island	180 (100)	10a, 10b			177 (98.3)			*3 (1.7)*			
BTA[1]+PIC+TB	Island arc	19	10c, 10d		10	6		*3*				
BSN+BTA[1]+TB+PIC	The Andes	51 (100)	10c, 10d		22 (43.1)	25 (49.0)		*3 (5.9)*	*1 (2.0)*			
BSN+BTA[1]+PHT+TB	MVB	45 (100)	10c, 10d		19 (42.2)	24 (53.3)		*2 (4.4)*				
BSN+BTA[1]+PHT+PIC+TB	Continental rift	134 (100)	10c, 10d		20 (14.9)	106 (79.1)		*2 (1.5)*	*6 (4.5)*			
BTA[2]+T+TA	Island arc	18 (100)	10e, 10f		*3*	*6*		3	5		1	
BTA[2]+T+TA	The Andes	70 (100)	10e, 10f		*2 (2.9)*	*6 (8.6)*		22 (31.4)	18 (25.7)		19 (27.1)	3 (4.3)
BTA[2]+T+TA	MVB	94 (100)	10e, 10f		*14 (14.9)*	*9 (9.6)*		38 (40.4)	24 (25.5)		7 (7.4)	2 (2.1)
BTA[2]+PH+PHT+TPH+TA	Continental rift	67 (100)	10e, 10f		*4 (6.0)*	*30 (44.8)*		3 (4.5)	17 (25.4)		4 (6.0)	9 (13.4)
BTA[2]+T+TA	Ocean Island	29 (100)	10e, 10f			*15 (52)*			11 (38)			3 (10)

The rock abbreviations are (see Verma *et al.* 2002): B,subalk– subalkali basalt; B,alk– alkali basalt; BTA[1]– basaltic trachyandesite (basic); PIC– picrite; TB– trachybasalt; BSN– basanite; PHT– phonotephrite; FOI– foidite; TEP– tephrite; PB– picrobasalt; BTA[2]– basaltic trachyandesite (intermediate); T– trachyte; TA– trachyandesite; PH– phonolite; TPH– tephtiphonolite; BA– basaltic andesite; A– andesite; D– dacite; TD– trachydacite; R– rhyolite. For the Co– Th diagram (Hastie *et al.* 2007), B– basalt; BA/A– basaltic andesita/andesita; D/R*– diorite/rhyolite/latite/trachyte; Thol.– tholeiite; CA– calc-alkaline; SHO– high-K and shoshonite. The percentages for total number of samples < 50 were arbitrarily quoted as integers. Numbers and percentages in boldface are for "obvious misclassification", also called "minimum misclassification" and those without boldface are correct rock name (not necessarily for the correct classification or success rate). The numbers and percentages in italic are for probable "minimum mis-classification". Note this highlighting is reverse to that used in Tables 1 and 2.

19 samples of such basic magmas from island arc setting were misclassified as basaltic andesite/andesite (Figure 10d), and 9 out of 18 intermediate magmas did so as basalt (Figure 10f).

Only continental rift and ocean island settings provided a statistically significant number of samples of ultrabasic magmas having both Co and Th data (Figure 10a). Mostly plotted as shoshonitic basalt (Figure 10b; Table 3), but a considerable number (22 out of 86 samples; 25.6%) from continental rifts were also classified as calc-alkaline basalt. The minimum misclassification was only three samples (1.7%), misclassified as basaltic andesite/andesite from an ocean island setting (Table 3). The minimum misclassification for basic magmas is represented by the few samples that are classified as basaltic andesite/andesite in the Co-Th diagram (Figure 10d; Table 3). They represent only about 4.4% to 7.9%. Similarly, for intermediate to acid magmas, the misclassified samples are those that plot as basalt (Figure 10f; Table 3). However, these are much more numerous than those for the earlier two categories. The minimum misclassification amounted to about 11.5%, 24.5%, 50.8%, and 52%, respectively, for the Andes, MVB, continental rifts, and ocean islands (Figure 10f; Table 3).

In summary, the minimum misclassification for those rock samples that have names common to the IUGS scheme and Co-Th diagram of Hastie *et al.* (2007) ranged as follows: (i) two cases of low values of about 1.2% and 8%; (ii) five cases of intermediate values of about 12.8–24.0%; (iii) seven cases of unacceptably high values of about 25.3–93% (see the upper part of Table 3). For those rocks with names in the IUGS scheme and not in the Co-Th diagram of Hastie *et al.* (2007), minimum misclassifications were generally small (1.7–11.5%), but with some greater values in the range of 24.5–52%.

Discussion: the Need of Still Newer Classification Diagram

On the basis of unacceptably low success rates for correct classification by the old W&F diagram and unacceptably high minimum misclassification registered for the new Hastie *et al.* (2007) diagram, we can safely conclude that both diagrams are flawed for the classification of altered rocks.

It is not clear to us how to employ the Co-Th diagram (Hastie *et al.* 2007), not much used so far by other researchers, for classification. The diagram is supposedly intended to discriminate altered arc volcanic rocks. In older terrains, where classification of altered rocks is badly needed, it seems to us that the user must first ascertain that the rocks actually belonged to an arc before using this diagram. If so, how is it to going to be done; by plate tectonic reconstructions or by discrimination diagrams? Plate reconstructions are largely model-based. Should we use discrimination diagrams? But, most existing discrimination diagrams do not work properly, as shown by one of us in a companion paper (Verma 2010). So, should we use only the new discriminant function discrimination diagrams (Agrawal *et al.* 2008) based on natural log-ratio transformation of relatively immobile elements?

The other question that arises is: is there any use in discriminating only three classes of rock names, two of which are largely indeterminate ('basaltic andesite/andesite' and 'dacite / rhyolite / latite / trachyte'), with two or more rock names in each of them? For fresh rocks there are a dozen of these individual names proposed by the IUGS (Le Bas *et al.* 1986; Le Bas 2000). Hence, the main use of this new Co-Th diagram is probably its capacity to assign tholeiitic, calc-alkaline and shoshonitic adjectives to basalt, basaltic andesite/andesite, and dacite/rhyolite/latite/trachyte.

From this discussion, it becomes clear to us that much work is needed in order to reach the goal of altered rock classification system that would better match the IUGS scheme. Floyd & Winchester (1975, 1978) and Winchester & Floyd (1976, 1977) attempted this even before the IUGS acceptance of the TAS diagram (Le Bas *et al.* 1986). However, the recent attempt (Hastie *et al.* 2007) does not provide us with a much needed working framework for classification of altered volcanic rocks from all tectonic settings either. Unfortunately, we are probably far from having 'a reliable way to classify rocks from the geological record'. Thus, new proposals for altered rock classification to solve the classification and nomenclature problems in earth sciences are badly needed.

Statistical Requirements for New Proposals

A major problem with bivariate (such as the Co-Th diagram of Hastie *et al.* 2007), ternary diagrams (such as those evaluated by Verma 2010) and even the element ratio/ratio plot (such as the Nb/Y-Zr/TiO_2 diagram of Winchester & Floyd 1977), is that they probably represent too few chemical variables to correctly handle the multivariate problem of altered rock classification. The closure and constant sum problem is another factor that inhibits correct statistical treatment (Chayes 1960, 1965, 1978; Aitchison 1984, 1986, 1989). The representativeness of the initial datasets used for proposing these various diagrams may be another factor that affects their application. In such diagrams the dividing boundaries are also subjective, generally drawn by eye. An objective way to replace them by probability-based boundaries has already been proposed (Agrawal 1999) and practiced in discrimination diagrams (Agrawal *et al.* 2004, 2008; Verma *et al.* 2006; Agrawal & Verma 2007).

In future we propose to follow the example of Verma *et al.* (2006) and Agrawal *et al.* (2008), who solved most of these problems by proposing new natural logarithm-ratio based discriminant function diagrams for tectonomagmatic discrimination using major- and trace-elements, respectively (Verma 2010). In addition to the above problems, statistical analysis also requires that the data be normally distributed without any discernible statistical contamination. Fortunately, this final problem can also be solved by the methodology proposed by Barnett & Lewis (1994) and considerably improved recently by Verma & Quiroz-Ruiz (2006a, 2006b, 2008), Verma *et al.* (2008b), and Verma (2009b, c). Such a statistical procedure of discordancy tests has been already extensively employed by numerous researchers (e.g., Castrellon-Uribe *et al.* 2008; Díaz-González *et al.* 2008; Jafarzadeh & Hosseini-Barzi 2008; Nagarajan *et al.* 2008; Obeidat *et al.* 2008; Palabiyik & Serpen 2008; Vargas-Rodríguez *et al.* 2008; Vattuone *et al.* 2008; Armstrong-Altrin 2009; Marroquín-Guerra *et al.* 2009; Pandarinath 2009a, b; Gómez-Arias *et al.* 2009; González-Márquez & Hansen 2009; González-Ramírez *et al.* 2009; Madhavaraju & Lee 2009; Ostrooumov *et al.* 2009; Rodríguez-Ríos & Torres-Aguilera 2009; Verma *et al.* 2009a, b). Therefore, it will not be difficult to incorporate this procedure in the production of new classification diagrams for altered volcanic rocks. Such combined methodology of extensive database, discordant outlier tests, and linear discriminant analysis could therefore be easily extended for the proposal of much needed new diagrams for plutonic rocks as well. This work is currently in progress.

Conclusions

From the statistical evaluations using fresh rocks presented in this work, we conclude that none of the existing classification diagrams works well for altered volcanic rocks. Therefore, an urgent need exists to explore this field of earth sciences and fulfil the much needed altered rock classification system. Significant progress has been achieved using statistical methods to identify discordant outliers, and linear discriminant analysis based on natural logarithm-ratio transformations, whose application would facilitate the proposal of new classification diagrams consistent with the IUGS nomenclature.

Acknowledgements

R. González-Ramírez expresses her gratitude to the Secretaría de Educación Pública for permission to carry out doctoral studies in Universidad Nacional Autónoma de México. R. Rodríguez-Ríos is grateful to the Universidad Autónoma de San Luis Potosí for granting him sabbatical leave to work at the Centro de Investigación en Energía (Universidad Nacional Autónoma de México). We are grateful to Samuele Agostini, an anonymous referee, and the editor Erdin Bozkurt, who all, while highly appreciating our work, provided suggestions that helped improve our presentation. We express our great sorrow to inform to the community that our colleague Rodolfo Rodríguez Ríos – coauthor of this paper – died on July 27, 2009. John A. Winchester edited English of the final text and Yalçın Ersoy translated the abstract to Turkish.

References

Agrawal, S. 1999. Geochemical discrimination diagrams: a simple way of replacing eye-fitted boundaries with probability based classifier surfaces. *Journal of the Geological Society of India* **54**, 335–346.

Agrawal, S. & Verma, S.P. 2007. Comment on 'Tectonic classification of basalts with classification trees' by Pieter Vermeesch (2006). *Geochimica et Cosmochimica Acta* **71**, 3388–3390.

Agrawal, S., Guevara, M. & Verma, S.P. 2004. Discriminant analysis applied to establish major-element field boundaries for tectonic varieties of basic rocks. *International Geology Review* **46**, 575–594.

Agrawal, S., Guevara, M. & Verma, S.P. 2008. Tectonic discrimination of basic and ultrabasic rocks through log-transformed ratios of immobile trace elements. *International Geology Review* **50**, 1057–1079.

Ahmad, T., Tanaka, T., Sachan, H.K., Asahara, Y., Islam, R. & Khanna, P.P. 2008. Geochemical and isotopic constraints on the age and origin of the Nidar Ophiolitic Complex, Ladakh, India: implications for the Neo-Tethyan subduction along the Indus suture zone. *Tectonophysics* **451**, 206–224.

Aitchison, J. 1984. Reducing the dimensionality of compositional data set. *Mathematical Geology* **16**, 617–635.

Aitchison, J. 1986. *The Statistical Analysis of Compositional Data*. Chapman and Hall, London New York.

Aitchison, J. 1989. Measures of location of compositional data sets. *Mathematical Geology* **21**, 787–790.

Armstrong-Altrin, J.S. 2009. Provenance of felsic beach sands from Cazones, Acapulco and Bahia Kino beaches, Mexico. *Revista Mexicana de Ciencias Geológicas* **26**, 764–782.

Bağci, U., Parlak, O. & Höck, V. 2008. Geochemistry and tectonic environment of diverse magma generations forming the crustal units of the Kızıldağ (Hatay) ophiolite, southern Turkey. *Turkish Journal of Earth Sciences* **17**, 43–71.

Barnett, V. & Lewis, T. 1994. *Outliers in Statistical Data*. John Wiley & Sons, Chichester.

Castrellon-Uribe, J., Cuevas-Arteaga, C. & Trujillo-Estrada, A. 2008. Corrosion monitoring of stainless steel 304L in lithium bromide aqueous solution using transmittance optical detection technique. *Optics and Lasers in Engineering* **46**, 469–476.

Chayes, F. 1960. On correlation between variables of constant sum. *Journal of Geophysical Research* **65**, 4185–4193.

Chayes, F. 1965. Classification in a ternary-diagram by means of discriminant functions. *American Mineralogist* **50**, 1618–1633.

Chayes, F. 1978. *Ratio Correlation. A Manual for Students of Petrology and Geochemistry*. The University of Chicago Press, Chicago and London.

Díaz-González, L., Santoyo, E. & Reyes-Reyes J. 2008. Tres nuevos geotermómetros mejorados de Na/K usando herramientas computacionales y geoquimiométricas: aplicación a la predicción de temperaturas de sistemas geotérmicos. *Revista Mexicana de Ciencias Geológicas* **25**, 465–482.

Floyd, P.A. & Winchester, J.A. 1975. Magma type and tectonic setting discrimination using immobile elements. *Earth and Planetary Science Letters* **27**, 211–218.

Floyd, P.A. & Winchester, J.A. 1978. Identification and discrimination of altered and meta-morphosed volcanic rocks using immobile elements. *Chemical Geology* **21**, 291–306.

Fournier, R.O. & Potter ii, R.W. 1982. A revised and expanded silica (quartz) geothermometer. *Geothermal Resources Council Bulletin* **11**, 3–12.

Gladkochub, D.P., Mazukabzov, A.M., Donskaya, T.V., De Waele, B., Stanevich, M. & Pisarevsky, S.A. 2008. The age and origin of volcanics in the Riphean section of the Siberian craton (western Baikal area). *Russian Geology and Geophysics* **49**, 749–758.

Gökten, E. & Floyd, P.A. 2007. Stratigraphy and geochemistry of pillow basalts within the ophiolitic melange of the İzmir-Ankara-Erzincan suture zone: implications for the geotectonic character of the northern branch of Neotethys. *International Journal of Earth Sciences* **96**, 725–741.

Gómez-Arias, E., Andaverde, J., Santoyo, E. & Urquiza, G. 2009. Determinación de la viscosidad y su incertidumbre en fluidos de perforación usados en la construcción de pozos geotérmicos: aplicación en el campo de Los Humeros, Puebla, México. *Revista Mexicana de Ciencias Geológicas* **26**, 516–529.

González-Márquez, L.C. & Hansen, A.M. 2009. Adsorción y mineralización de atrazina y relación con parámetros de suelos del DR 063 Guasave, Sinaloa. *Revista Mexicana de Ciencias Geológicas* **26**, 587–599.

González-Ramírez, R., Díaz-González, L. & Verma, S.P. 2009. Eficiencia relativa de las 33 pruebas de discordancia para valores desviados basada en datos geoquímicos de materiales de referencia. *Revista Mexicana de Ciencias Geológicas* **26**, 501–515.

Gürsü, S. 2008. Petrogenetic and tectonic significance of rift-related pre-Early Cambrian mafic dikes, Central Taurides, Turkey. *International Geology Review* **50**, 895–913.

Hastie, A.R., Kerr, A.C., Pearce, J.A. & Mitchell, S.F. 2007. Classification of altered volcanic island rocks using immobile trace elements: development of the Th-Co discrimination diagram. *Journal of Petrology* **48**, 2341–2357.

Jafarzadeh, M. & Hosseini-Barzi, M. 2008. Petrography and geochemistry of Ahwaz Sandstone Member of Asmari Formation, Zagros, Iran: implications on provenance and tectonic setting. *Revista Mexicana de Ciencias Geológicas* **25**, 247–260.

Kadir, S., Önen-Hall, A.P., Aydin, S.N., Yakicier, C., Akarsu, N. & Tuncer, M. 2008. Environmental effect and genetic influence: a regional cancer predisposition survey in the Zonguldak region of Northwest Turkey. *Environmental Geology* **54**, 391–409.

Keskin, M., Genç, Ş.C. & Tüysüz, O. 2008. Petrology and geochemistry of post-collisional Middle Eocene volcanic units in North-Central Turkey: evidence for magma generation by slab breakoff following the closure of the Northern Neotethys Ocean. *Lithos* **104**, 267–305.

Kalmar, J. & Kovacs-Palffy, P. 2008. Geochemical study of leptinites from Stejera (Romania). *Carpathian Journal of Earth and Environmental Sciences* **3**, 49–64.

Kaygusuz, A., Siebel, W., Şen, C. & Satir, M. 2008. Petrochemistry and petrology of I-type granitoids in an arc setting: the composite Torul pluton, Eastern Pontides, NE Turkey. *International Journal of Earth Sciences* **97**, 739–764.

Le Bas, M.J. 2000. IUGS reclassification of the high-Mg and picritic volcanic rocks. *Journal of Petrology* **41**, 1467–1470.

Le Bas, M.J., Le Maitre, R.W., Streckeisen, A. & Zanettin, B. 1986. A chemical classification of volcanic rocks based on the total alkali-silica diagram. *Journal of Petrology* **27**, 745–750.

Le Maitre, R.W., Streckeisen, A., Zanettin, B., Le Bas, M.J., Bonin, B., Bateman, P., Bellieni, G., Dudek, A., Schmid, R., Sorensen, H. & Woolley, A.R. 2002. *Igneous Rocks. A Classification and Glossary of Terms: Recommendations of the International Union of Geological Sciences Subcommission of the Systematics of Igneous Rocks*. Cambridge University Press, Cambridge.

Madhavaraju, J. & Lee, Y.I. 2009. Geochemistry of the Dalmiapuram Formation of the Uttatur Group (Early Cretaceous), Cauvery basin, southeastern India: Implications on Provenance and Paleo-redox conditions. *Revista Mexicana de Ciencias Geológicas* **26**, 380–394.

Marroquín-Guerra, S.G., Velasco-Tapia, F. & Díaz-González, L. 2009. Evaluación estadística de Materiales de Referencia Geoquímica del Centre de Recherches Pétrographiques et Géochimiques (Francia) aplicando un esquema de detección y eliminación de valores desviados y su posible aplicación en el control de calidad de datos geoquímicas. *Revista Mexicana de Ciencias Geológicas* **26**, 530–542.

Mondal, M.E.A., Chandra, R. & Ahmad, T. 2008. Precambrian mafic magmatism in Bundelkhand craton. *Journal of the Geological Society of India* **72**, 113–122.

Nagarajan, R., Sial, A.N., Armstrong-Altrin, J.S., Madhavaraju, J. & Nagendra, R. 2008. Carbon and oxygen isotope geochemistry of Neoproterozoic limestones of the Shahabad Formation, Bhima basin, Karnataka, southern India. *Revista Mexicana de Ciencias Geológicas* **25**, 225–235.

Nardi, L.V.S., Pla-Cid, J., Bitencourt, M.D. & Stabel, L.Z. 2008. Geochemistry and petrogenesis of post-collisional ultrapotassic syenites and granites from southernmost Brazil: the Piquiri Syenite Massif. *Anais da Academia Brasileira de Ciencias* **80**, 353–371.

Obeidat, M.M., Ahmad, F.Y., Hamouri, N.A.A., Massadeh, A.M. & Athamneh, F.S. 2008. Assessment of nitrate contamination of karst springs, Bani Kanana, Northern Jordan. *Revista Mexicana de Ciencias Geológicas* **25**, 426–437.

Ostrooumov, M., Taran, Y., Arellano-Jiménez, M., Ponce, A. & Reyes-Gasga, J. 2009. Colimaite, K3VS4 – a new potassium-vanadium sulfide mineral from the Colima volcano, State of Colima (Mexico). *Revista Mexicana de Ciencias Geológicas* **26**, 600–608.

Palabiyik, Y. & Serpen, U. 2008. Geochemical assessment of Simav geothermal field, Turkey. *Revista Mexicana de Ciencias Geológicas* **25**, 408–425.

Pandarinath, K. 2009a. Clay minerals in SW Indian continental shelf sediments cores as indicators of provenance and paleomonsoonal conditions: a statistical approach. *International Geology Review* **51**, 145–165.

Pandarinath, K. 2009b. Evaluation of geochemical sedimentary reference materials of the Geological Society of Japan (GSJ) by an objective outlier rejection statistical method. *Revista Mexicana de Ciencias Geológicas* **26**, 638–646.

Pandarinath, K., Pushparani, D.E., Torres-Alvarado, I. & Verma, S.P. 2006. X-ray diffraction analysis of hydrothermal minerals from the Los Azufres geothermal system, Mexico. *International Geology Review* **48**, 174–190.

Pandarinath, K., Duski, P., Torres-Alvarado, I.S. & Verma, S.P. 2008. Element mobility during the hydrothermal alteration of rhyolitic rocks of the Los Azufres geothermal field, Mexico. *Geothermics* **37**, 53–72.

Peccerillo, A. & Taylor, S.R. 1976. Geochemistry of Eocene calc-alkaline volcanic rocks from the Kastamonu area, Northern Turkey. *Contributions to Mineralogy and Petrology* **58**, 63–81.

Rodríguez-Ríos, R. & Torres-Aguilera, J.M. 2009. Evolución petrológica y geoquímica de un vulcanismo bimodal oligocénico en el Campo Volcánico de San Luis Potosí (México). *Revista Mexicana de Ciencias Geológicas* 26, 658–673.

Shekhawat, L.S., Pandit, M.K. & Joshi, D.W. 2007. Geology and geochemistry of palaeoproterozoic low-grade metabasic volcanic rocks from Salumber area, Aravalli Supergroup, NW India. *Journal of Earth System Science* **116**, 511–524.

Sheth, H.C. & Melluso, L. 2008. The Mount Pavagadh volcanic suite, Deccan Traps: Geochemical stratigraphy and magmatic evolution. *Journal of Asian Earth Sciences* **32**, 5–21.

Torres-Alvarado, I.S. 2002. Chemical equilibrium in hydrothermal systems: the case of Los Azufres geothermal field, Mexico. *International Geology Review* **44**, 639–652.

Torres-Alvarado, I.S., Pandarinath, K., Verma, S.P. & Dulski, P. 2007. Mineralogical and geochemical effects due to hydrothermal alteration in the Los Azufres geothermal field, Mexico. *Revista Mexicana de Ciencias Geológicas* **24**, 15–24.

Vargas-Rodríguez, Y.M., Gómez-Vidales, V., Vázquez-Labastida E., García-Borquez, A., Aguilar-Sahagun, G., Murrieta-Sánchez, H. & Salmon, M. 2008. Caracterización espectroscópica, química y morfológica y propiedades superficiales de una montmorillonita Mexicana. *Revista Mexicana de Ciencias Geológicas* **25**, 135–144.

Vasconcelos-F.M., Verma, S.P. & Rodríguez-G., J.F. 1998. Discriminación tectónica: nuevo diagrama Nb-Ba para arcos continentales, arcos insulares, 'rifts' e islas oceánicas en rocas máficas. *Boletín de la Sociedad Española de Mineralogía* **21**, 129–146.

Vasconcelos-F.M., Verma, S.P. & Vargas-B., R.C. 2001. Diagrama Ti-V: una nueva propuesta de discriminación para magmas básicos en cinco ambientes tectónicos. *Revista Mexicana de Ciencias Geológicas* **18**, 162–174.

Vattuone, M.E., Leal, P.R., Crosta, S., Berbeglia, Y., Gallegos, E. & Martínez-Dopico, C. 2008. Paragénesis de zeolitas alcalinas en un afloramiento de basaltos olivínicos amigdaloides de Junín de Los Andes, Neuquén, Patagonia, Argentina. *Revista Mexicana de Ciencias Geológicas* **25**, 483–493.

Verma, S.P. 1997. Estado actual de los diagramas de clasificación magmática y de discriminación tectónica. *Actas INAGEQ* **3**, 49–78.

Verma, M.P. 2000a. Revised quartz solubility temperature dependence equation along the water-vapor saturation curve. *Proceedings World Geothermal Congress, Kyushu-Tohoku, Japan*, 1927–1932.

Verma, S.P. 2000b. Geochemistry of the subducting Cocos plate and the origin of subduction-unrelated mafic volcanism at the volcanic front of the central Mexican Volcanic Belt. *In*: Delgado-Granados, H., Aguirre-Díaz, G. & Stock, J. M. (eds), *Cenozoic Tectonics and Volcanism of Mexico*. Geological Soceity of America, Geological Society of America Special Paper **334**, 195–222.

Verma, S.P. 2002. Absence of Cocos plate subduction-related basic volcanism in southern Mexico: a unique case on Earth? *Geology* **30**, 1095–1098.

Verma, S.P. 2004. Solely extension-related origin of the eastern to west-central Mexican Volcanic Belt (Mexico) from partial melting inversion model. *Current Science* **86**, 713–719.

Verma, S.P. 2006. Extension related origin of magmas from a garnet-bearing source in the Los Tuxtlas volcanic field, Mexico. *International Journal of Earth Sciences* **95**, 871–901.

Verma, S.P. 2009a. Continental rift setting for the central part of the Mexican Volcanic Belt: A Statistical Approach. *The Open Geology Journal* **3**, 8–29.

Verma, S.P. 2009b. Evaluation of polynomial regression models for the Student t and Fisher F critical values, the best interpolation equations from double and triple natural logarithm transformation of degrees of freedom up to 1000, and their applications to quality control in science and engineering. *Revista Mexicana de Ciencias Geológicas* **26**, 79–92.

Verma, S.P. 2010. Statistical evaluation of bivariate, ternary and discriminant function tectonomagmatic discrimination diagrams. *Turkish Journal of Earth Sciences* **19**, 185–238.

Verma, S.P. & Aguilar-y-Vargas, V.H. 1988. Bulk chemical composition of magmas in the Mexican Volcanic Belt (Mexico) and inapplicability of generalized arc-models. *Chemie der Erde* **48**, 203–221.

Verma, S.P. & Quiroz-Ruiz, A. 2006a. Critical values for six Dixon tests for outliers in normal samples up to sizes 100, and applications in science and engineering. *Revista Mexicana de Ciencias Geológicas* **23**, 133–161.

Verma, S.P. & Quiroz-Ruiz, A. 2006b. Critical values for 22 discordancy test variants for outliers in normal samples up to sizes 100, and applications in science and engineering. *Revista Mexicana de Ciencias Geológicas* **23**, 302–319.

Verma, S.P. & Quiroz-Ruiz, A. 2008. Critical values for 33 discordancy test variants for outliers in normal samples for very large sizes of 1,000 to 30,000 and evaluation of different regression models for the interpolation and extrapolation of critical values. *Revista Mexicana de Ciencias Geológicas* **25**, 369–381.

Verma, S.P. & Santoyo, E. 1997. New improved equations for Na/K, Na/Li and SiO_2 geothermometers by outlier detection and rejection. *Journal of Volcanology and Geothermal Research* **79**, 9–23.

Verma, S.P., Guevara, M. & Agrawal, S. 2006. Discriminating four tectonic settings: five new geochemical diagrams for basic and ultrabasic volcanic rocks based on log-ratio transformation of major-element data. *Journal of Earth System Science* **115**, 485–528.

Verma, S.P., Torres-Alvarado, I.S. & Sotelo-Rodríguez, Z.T. 2002. SINCLAS: standard igneous norm and volcanic rock classification system. *Computers & Geosciences* **28**, 711–715.

Verma, S.P., Torres-Alvarado, I.S. & Velasco-Tapia, F. 2003. A revised CIPW norm. *Schweizerische Mineralogische und Petrographische Mitteilungen* **83**, 197–216.

Verma, S.P., Pandarinath, K. & Santoyo, E. 2008a. SolGeo: A new computer program for solute geothermometers and its application to Mexican geothermal fields. *Geothermic* **37**, 597–621.

Verma, S.P. & Quiroz-Ruiz, A. & Díaz-González. L. 2008b Critical values for 33 discordancy test variants for outliers in normal samples up to sizes 1000, and applications in quality control in Earth Sciences. *Revista Mexicana de Ciencias Geológicas* **25**, 82–96.

Verma, S.P., Díaz-González. L. & González-Ramírez, R. 2009a. Relative efficiency of single-outlier discordancy tests for processing geochemical data on reference materials and application to instrumental calibrations by a weighted least-squares linear regression model. *Geostandards and Geoanalytical Research* **33**, 29–49.

Verma, S.P., Pandarinath, K., Velasco-Tapia, F. & Rodríguez-Ríos, R. 2009b. Evaluation of the odd-even effect in limits of detection for electron microprobe analysis of natural minerals. Analytica Chimica Acta **638**, 126–132.

Wang, X.C., Li, X.H., Li, W.X., Li, Z.X., Liu, Y., Yang, Y.H., Liang, X.R. & Tu, X.L. 2008. The Bikou basalts in the northwestern Yangtze block, South China: Remnants of 820–810 Ma continental flood basalts? *Geological Society of America Bulletin* **120**, 1478–1492.

Winchester, J.A. & Floyd, P.A. 1976. Geochemical magma type discrimination: application to altered and metamorphosed basic igneous rocks. *Earth and Planetary Science Letters* **28**, 459–469.

Winchester, J.A. & Floyd, P.A. 1977. Geochemical discrimination of different magma series and their differentiation products using immobile elements. *Chemical Geology* **20**, 325–343.

Yiğitbaş, E., Winchester, J.A. & Ottley, C.J. 2008. The geochemistry and setting of the Demirci paragneisses of the Sunnice Massif, NW Turkey. *Turkish Journal of Earth Sciences* **17**, 421–431.

Zheng, Y., Gu, L., Tang, X., Li, C., Liu, S. & ChangZhi, W. 2008. Geological and geochemical signature of sea-floor alteration rocks of the highly metamorphosed Hongtoushan massive sulfide deposite, Liaoning. *Acta Petrologica Sinica* **24**, 1928–1936.